Supplementary Information

Bimetallic Pd/Cu complexes of pyridylchalcogenolates and catalytic activity in Sonogashira reaction

M. K. Pal[a], A. P. Wadawale[a] and S. Dey[a,b,*]

[a] Chemistry Division, Bhabha Atomic Research Centre, Mumbai 400 085, India

[b] Homi Bhabha National Institute, Training School Complex, Mumbai-400094, India

** E-mail: dsandip@barc.gov.in (S. Dey); Tel: +91-22-2559-2589*

Materials and methods

All experiments were carried out under a nitrogen atmosphere by using standard Schlenk technique. Solvents used in the reactions were degassed with nitrogen and distilled using standard procedures. The 4,4′-dipyridyldisulfide (4,4́-py_2S_2) was used as purchased from commercial sources without further purification. The ligand 4,4′-dipyridyldiselenide (4,4́-py_2Se_2[1] and the complexes $[PdCl(4\text{-}Sepy)]_n$ and $[PdCl(PPh_3)_2(4\text{-}Sepy)]$ were prepared by literature methods.[2] Melting points were determined in capillary tubes and are uncorrected. Elemental analyses were carried out on a Thermo Fischer Flash EA1112 CHNS analyzer. ^{1}H NMR spectra were recorded on a Bruker NMR spectrometers operating at 300 MHz, chemical shifts are relative to internal chloroform-d_1 peak (δ 7.26). For $^{31}P\{^1H\}$ NMR spectra were recorded on NMR spectrometer operating at 121.5 MHz. Mass spectra were recorded on a maXis Impact (Bruker) mass spectrometer. Thermo gravimetric analyses (TGA) were carried out on a Nitzsch STA 409 PC-Luxx TG-DTA instrument, which was calibrated with $CaC_2O_4.H_2O$. The TG curves were recorded at a heating rate of 10 ^{0}C min^{-1} under a flow of argon. ESCA apparatus (SPECS GmbH) with an Al-K_α (1486.6 eV) X-ray Source was

deployed for XPS measurements. The binding energy was calibrated using Au-4$f_{7/2}$ line (83.95 eV) and corrected using C 1 s line (284.5 eV) from adventitious aliphatic carbon.

Synthesis of complexes:

[{PdCl(4-Spy)]$_n$

A methanolic solution (10 mL) of Na_2PdCl_4 (395 mg, 1.34 mmol) was added to a freshly prepared methanolic solution (15 mL) of Na(4-SC_5H_4N) (prepared from 4,4′-$(C_5H_4N)_2S_2$ (148 mg, 0.67 mmol) and $NaBH_4$ (51 mg, 1.35 mmol)) with stirring which continued for 6 h at room temperature afforded a dark brown precipitate. The brown precipitate was filtered through a G3 assembly and washed with water, acetone and diethyl ether and dried in vacuo (320 mg, 95%). M.p. >200 °C. Anal. Calcd for C_5H_4NPdCl: C, 23.83; H, 1.60; N, 5.56; Found: C, 23.94; H, 1.69; N, 5.31.

[{PdCl(PPh$_3$)$_2$(4-Spy)] (1a)

To dichloromethane suspension (20 mL) of [PdCl(4-Spy)]$_n$ (188.8 mg, 0.085 mmol), solid PPh_3 (393.0 mg, 1.498 mmol) was added with stirring. The dark-red solution was stirred for 6 h at room temperature. The solvents were evaporated using vacuum, the brown residue was washed with diethyl ether, extracted with acetone (3 × 6 mL) and filtered. The filtrate was concentrated to 10 mL and kept in refrigerator to yield red crystals of the title complex (442.0 mg, 76 %), m.p. 156 ºC. Anal. Calcd for $C_{41}H_{34}ClNP_2PdS$: C, 63.41; H, 4.41; N, 1.80; Found: C, 63.52; H, 4.29; N, 1.67%. ^{1}H NMR ($CDCl_3$): δ 7.66–7.60 (m, 14H, *o*-H, Ph and 2,6-H, py), 7.39–7.31 (m, 18H, *m/p*-H, Ph), 6.87 (br, 2H, 3,5-H, py); ^{31}P{^{1}H} NMR ($CDCl_3$): δ 24.7 (s). Small amount of PPh_3 (δ −5.8) and $OPPh_3$ (δ 29.2) existed in solution.

[{Pd(PPh$_3$)$_2$(4-Spy)$_2$] (2a)

To methanolic solution (20 mL) of Na(4-SC_5H_4N) (prepared from 4,4′-$(C_5H_4N)_2S_2$ (72.6 mg, 0.33 mmol) and $NaBH_4$ (24.9 mg, 0.66 mmol)), solid $Pd(PPh_3)_2Cl_2$ (231.3 mg, 0.33 mmol) was

added with stirring. The orange coloured suspension was stirred for 3 h at room temperature. The whole reaction mixture was filtered through G-3 filtering assembly and the orange residue obtained was washed with hexane and diethyl ether (3 × 6 mL) to yield title complex (220.0 mg, 78 %), m.p. 182 ºC. The product was recrystallized from methanol solvent to get red crystals. ^{1}H NMR ($CDCl_3$): δ 8.16 (d, 4.1Hz, 2H, py), 7.83 (d, 5.5 Hz, 2H, py), 7.67 (d, 5.5Hz, 2H, py), 7.60–7.53 (m, 26H, *o*-H, Ph and py), 7.38–7.19 (m, 38H, *m/p*-H, Ph and py), 6.97 (d, 5.4Hz, 2H, py), 6.83 (d, 5.7Hz, 2H, py), 6.75 (d, 5.5Hz, 2H, py); ^{31}P{^{1}H} NMR ($CDCl_3$): δ 33.7 (s, dimeric complex), 25.1 (s, monomeric complex). Small amount of free PPh_3 (δ −5.4) existed in solution.

General experimental procedure for the catalysis reaction:

In an oven dried 25 ml Schlenk flask, a mixture of aryl halide (1 mmol), phenylacetylene (1.2 mmol), Pd catalyst (0.1 mol%), Base (2 mmol) in 3 ml DMA was heated in an oil bath at 120 ºC for 15 h with continuous stirring. After 15 h the reaction mixture was cooled to room temperature and the product was extracted with ethyl acetate (3 x 5 ml). After drying over Na_2SO_4, the solvent was removed under vacuum, and the resulting crude product was purified by column chromatography on silica gel.

X-ray Crystallography

A Rigaku-Oxford make XtaLAB Synergy, Dualflex X-ray diffractometer was employed for crystal screening, unit cell determination, and data collection. The goniometer was controlled using the APEX3 software suite.[3] The X-ray radiation employed was generated from a Cu X-ray tube Kα (λ = 1.54184 Å). Integrated intensity information for each reflection was obtained by reduction of the data frames with the program APEX3.[3] The integration method employed a three-dimensional profiling algorithm and all data were corrected for Lorentz and polarization

factors, as well as for crystal decay effects. Finally, the data was merged and scaled to produce a suitable data set. The absorption correction program SADABS[4] was employed to correct the data for absorption effects. Systematic reflection conditions and statistical tests of the data suggested the space group *Cc*. A solution was obtained readily using XT/XS in APEX3.[3,5] Hydrogen atoms were placed in idealized positions and were set riding on the respective parent atoms. All non-hydrogen atoms were refined with anisotropic thermal parameters. The structure was refined (weighted least squares refinement on F^2) to convergence.[5,6] Olex2 was employed for the final data presentation and structure plots.[6]

References:

1. B. Boduszek and R. Gancarz, *J. Prakt. Chem.*, 1996, **338**, 186−189.
2. K. V. Vivekananda, S. Dey, A. Wadawale, N. Bhuvanesh, V. K. Jain, *Dalton Trans*., 2013, **42**, 14158.
3. APEX3 "Program for Data Collection on Area Detectors" BRUKER AXS Inc., 5465 East Cheryl Parkway, Madison, WI 53711−5373 USA.
4. G. M. Sheldrick, SADABS, "Program for Absorption Correction of Area Detector Frames", BRUKER AXS Inc., 5465 East Cheryl Parkway, Madison, WI 53711−5373 USA.
5. (a) G. M. Sheldrick, *Acta Cryst.*, 2008, **A64**, 112−122. (b) G. M. Sheldrick, *Acta Cryst.*, 2015, **A71**, 3−8. (c) G. M. Sheldrick, *Acta Cryst.*, 2015, **C71**, 3−8. XT, XS, BRUKER AXS Inc., 5465 East Cheryl Parkway, Madison, WI 53711−5373 USA.
6. O. V. Dolomanov, L. J. Bourhis, R. J. Gildea, J. A. K. Howard and H. Puschmann, "OLEX2: A Complete Structure Solution, Refinement and Analysis Program", *J. Appl. Cryst.,* 2009, **42**, 339−341.

Table S1 Mass data for [{$Pd(PPh_3)_2$(4-Spy)$_2$}{$Cu(PPh_3)_2Cl$}$_2$] (**3**).

Mass fragments of complex **3**	Isotopic mass, *m/z*	Calculated peak of the most abundant ion	Experimental peak of the most abundant ion
([M + CH_3CN – (2Cl + PPh_3 + 2py)]$^+$, 56%)	1729.24	1731.26	1731.09
([M + Na + CH_3CN – 9Ph)]$^+$, 98%)	1464.92	1468.95	1468.99
([M + CH_3CN – (Cl + 9Ph)]$^+$, 81%)	1406.97	1408.99	1408.99
([M + H – (Cl + 9Ph)]$^+$, 100%)	1366.95	1368.97	1369.10
([M + Na + 2CH_3CN – ($CuCl(PPh_3)_2$ + Cl + Spy + 2Ph)]$^+$, 100%)	1278.17	1280.18	1280.17
([M – (2Cl + 2PPh_3 + 3Ph)]$^+$, 74%)	1269.03	1271.04	1271.21

Table S2 Mass data for [{$Pd(PPh_3)_2$(4-Sepy)$_2$}{$Cu(PPh_3)_2Cl$}$_2$] (**4**).

Mass fragments of complex **4**	Isotopic mass, *m/z*	Calculated peak of the most abundant ion	Experimental peak of the most abundant ion
([M – (PPh_3 + 4Ph)]$^+$, 59%)	1619.90	1621.93	1622.03
([M + H – ($CuCl(PPh_3)_2$ + Ph)]$^+$, 37%)	1492.04	1492.06	1492.08
([M + Na – ($CuCl(PPh_3)_2$ + 3Ph)]$^+$, 100%)	1359.94	1359.96	1359.94

Table S3: Optimization of reaction parameters[a].

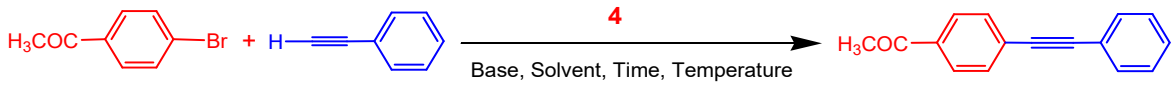

Entry	Base	Catalyst	Solvent	Time (h)	Temp. (°C)	Yield (%)
Effect of Base:						
1	Cs_2CO_3	**4**	DMSO	15	120	30
2	Et_3N	**4**	DMSO	15	120	-
3	K_2CO_3	**4**	DMSO	15	120	70
Effect of solvent:						
4	K_2CO_3	**4**	DMSO	15	120	70
5	K_2CO_3	**4**	dioxane	15	reflux	-
6	K_2CO_3	**4**	methanol	15	reflux	-
7	K_2CO_3	**4**	1,2-Dimethoxy ethane (DME)	15	reflux	-
8	K_2CO_3	**4**	DMF	15	120	40
9	K_2CO_3	**4**	Dimethyl acetamide (DMA)	15	120	80
Effect of time:						
10	K_2CO_3	**4**	DMA	3	120	19
11	K_2CO_3	**4**	DMA	6	120	38
12	K_2CO_3	**4**	DMA	10	120	57
13	K_2CO_3	**4**	DMA	12	120	69
14	K_2CO_3	**4**	DMA	15	120	80
15	K_2CO_3	**4**	DMA	20	120	80

[a] Reaction conditions: 4-bromoacetophenone (1 mmol), phenyl acetylene (1.2 mmol), base (2 mmol), catalyst **4** (0.1 mol % of Pd).

Table S4. Comparison of the results reported for different Pd-based heterobimetallic catalysts in the Sonogashira coupling reaction.

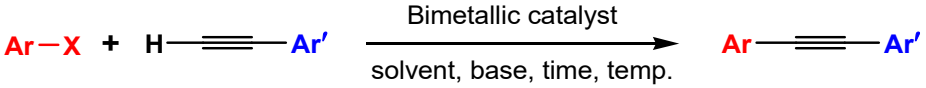

Entry	Ar–X	Ar′	Catalyst	mol% of "**Pd**"	Reaction conditions	% yield	Refs.
1	PhBr	Ph	**MnPdL3** complex (L3 = pyridine-hydrazone-pyrimidine- hydrazone-phosphane scaffolds)	6	CH_3CN, DABCO, 90 °C, 24h	59	38
2	PhBr	Ph	**CoPdL3** complex	6	CH_3CN, DABCO, 90 °C, 4h	99	38
3	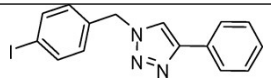	Ph	**$[PdCuL_2](PF_6)_3$** (L = 3-(1,10-phenanthrolin-2-yl)-1-(pyridin-2-ylmethyl)imidazolylidene)	0.01	DMF, pyrrolidine, 80 °C, 2h	86	39
4	$4\text{-}CH_3COC_6H_4Br$	Ph	**Pd^{II}/Ir^{III}** complex based on naphthalene and triazolylidene	1.0	DMF, KO^tBu, 100 °C, 4h	75[a]	40
5	PhI	Ph	**Pd^{II}/Cu^{I}-polymer complex** based on polyamic acid with biquinolyl group	0.1	NMP, Bu_3N, 100 °C, 5h	88	41
6	$4\text{-}MeC_6H_4Br$	Ph	**PdCu NPs supported on MgO**	0.02	DMF, DABCO, 80 °C, 24h	83	42
7	PhI	$SiMe_3$	**Pd-Cu/C**	10	MeOH, Et_2NH, 120 °C, 20 min	70	43
8	PhI	Ph	**Pd@HKUST-1@Cu^{II}/CMC** (CMC = carboxymethylcellulose)	0.42	DMSO, K_2CO_3, 90 °C, 6h	96	44
9	PhI	Ph	**Cu/Pd@Mod-PANI-3OH** (PANI = polyaniline)	0.09	H_2O, Et_3N, 80 °C, 24h	92	45
10	PhI	Ph	**Pd/Cu@MCC-PAMAMG2.5-PEI** (PAMAM = polyamidoamine; MCC = Microcrystalline cellulose)	0.65	DMSO, K_2CO_3, 100 °C, 4h	96	46
11	$4\text{-}CH_3COC_6H_4Br$	Ph	$[\{Pd(PPh_3)_2(4\text{-}Sepy)_2\}\{Cu(PPh_3)_2Cl\}_2]$	0.1	DMA, K_2CO_3, 120 °C, 15h	80	this work

[a]PPh_3 as additive.

Table S5 Crystallographic and structure refinement data for $[PdCl(PPh_3)_2(4\text{-Spy})]$ (**1a**) and $[Pd(PPh_3)_2(4\text{-Spy})_2].2CH_3OH$ (**2a**).

Compounds	$[PdCl(PPh_3)_2(4\text{-Spy})]$	$[Pd(PPh_3)_2(4\text{-Spy})_2].2CH_3OH$
Chemical Formula	$C_{41}H_{34}ClNP_2PdS$	$C_{48}H_{46}N_2O_2P_2PdS_2$
Formula weight	776.60	915.33
Crystal Size (mm^3)	0.50 x 0.50 x 0.50	0.100 x 0.040 x 0.020
T/K	298(2)	298(2)
λ/Å	CuKα (λ = 1.54184 Å)	CuKα (λ = 1.54184 Å)
Crystal system	Monoclinic	Monoclinic
Space group	C 2/c	P 21/c
a/Å	10.93610(10)	13.1283(2)
b/Å	16.70070(10)	19.3886(3)
c/Å	40.8473(4)	8.76560(10)
α/°	90	90
β/°	96.7350(10)	91.4320(10)
γ/°	90	90
V/$Å^3$	7408.89(11)	2230.49(5)
ρ_{calc}/g cm^{-3}	1.407	1.363
Z	8	2
μ/mm^{-1}	6.285	5.219
Reflection collected/ unique	17675/ 7339	16240/ 4504
Data/restraints/parameters	7339/ 114/ 465	4504/ 0/ 261
Final R_1, wR_2 indices	R1 = 0.0341, wR2 = 0.0928	R1 = 0.0353, wR2 = 0.0898
R_1, wR_2 (all data)	R1 = 0.0631, wR2 = 0.1107	R1 = 0.0572, wR2 = 0.1109
Largest diff. peak & hole [$eÅ^{-3}$]	1.164 and -1.929	0.912 and -1.148

Table S6 Crystallographic and structure refinement data for [{$Pd(PPh_3)_2$(4-Spy)$_2$}{$Cu(PPh_3)_2Cl$}$_2$] (**3**) and [{$Pd(PPh_3)_2$(4-Sepy)$_2$}{$Cu(PPh_3)_2Cl$}$_2$] (**4**)

Compounds	**3**	**4**
Chemical Formula	$C_{118}H_{98}Cl_2Cu_2N_2P_6PdS_2$	$C_{118}H_{98}Cl_2Cu_2N_2P_6PdSe_2$
Formula weight	2098.30	2192.10
Crystal Size (mm^3)	0.25 x 0.15 x 0.05	0.25 x 0.20 x 0.05
T/K	298(2)	298(2)
λ/Å	CuKα (λ = 1.54184 Å)	CuKα (λ = 1.54184 Å)
Crystal system	Triclinic	Triclinic
Space group	P -1	P -1
a/Å	11.68270(10)	12.3318(4)
b/Å	14.22020(10)	12.7988(5)
c/Å	16.74980(10)	19.1873(7)
α/°	69.4180(10)	81.853(3)
β/°	78.0530(10)	77.968(3)
γ/°	83.5570(10)	67.800(4)
V/$Å^3$	2546.24(4)	2735.65(19)
ρ_{calc}/g cm^{-3}	1.368	1.331
Z	1	1
μ/mm^{-1}	4.040	4.164
Reflection collected/ unique	24515/ 10386	24515/ 11074
Data/restraints/parameters	10386/ 0/ 602	11074/ 81/ 629
Final R_1, wR_2 indices	R1 = 0.0420, wR2 = 0.1063	R1 = 0.0467, wR2 = 0.1363
R_1, wR_2 (all data)	R1 = 0.0436, wR2 = 0.1075	R1 = 0.0531, wR2 = 0.1424
Largest diff. peak & hole [$eÅ^{-3}$]	1.673 and -0.962	0.944 and -0.792

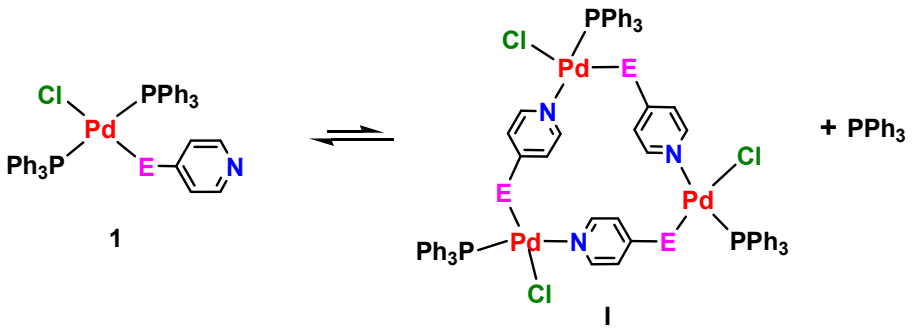

Scheme S1 Equilibria between monomeric complex **1** [PdCl(PPh_3)$_2$(4-Epy)] and trimeric complex [PdCl(PPh_3)(4-Sepy)]$_3$ (**I**).

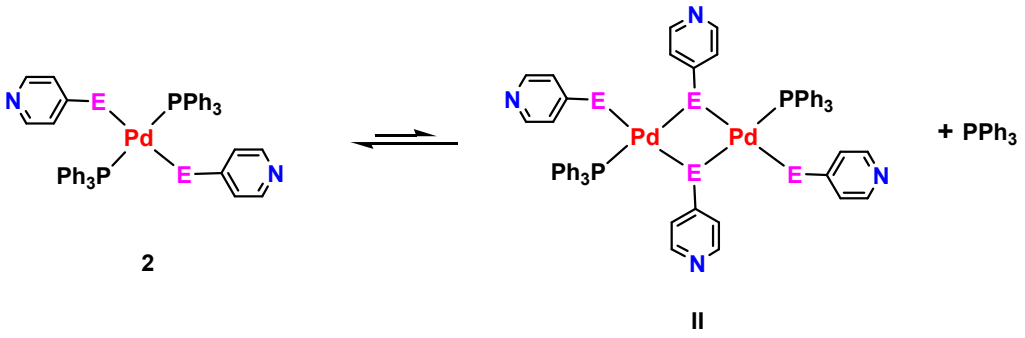

Scheme S2 Equilibria between monomeric complex **2** [Pd(PPh_3)$_2$(4-Epy)$_2$] and dimeric complex [Pd(PPh_3)(μ-4-Epy)(4-Epy)]$_2$ (**II**).

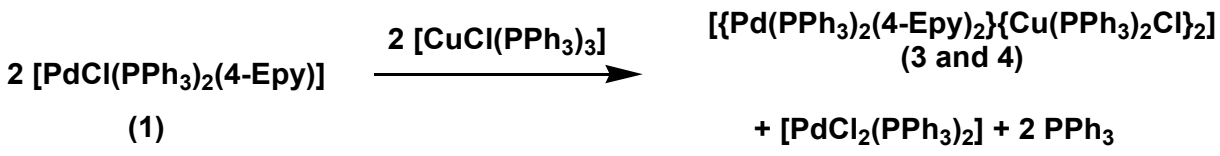

Scheme S3. Preparation of **3** and **4** [{Pd(PPh_3)$_2$(4-Sepy)$_2$}{Cu(PPh_3)$_2$Cl}$_2$] via route i.

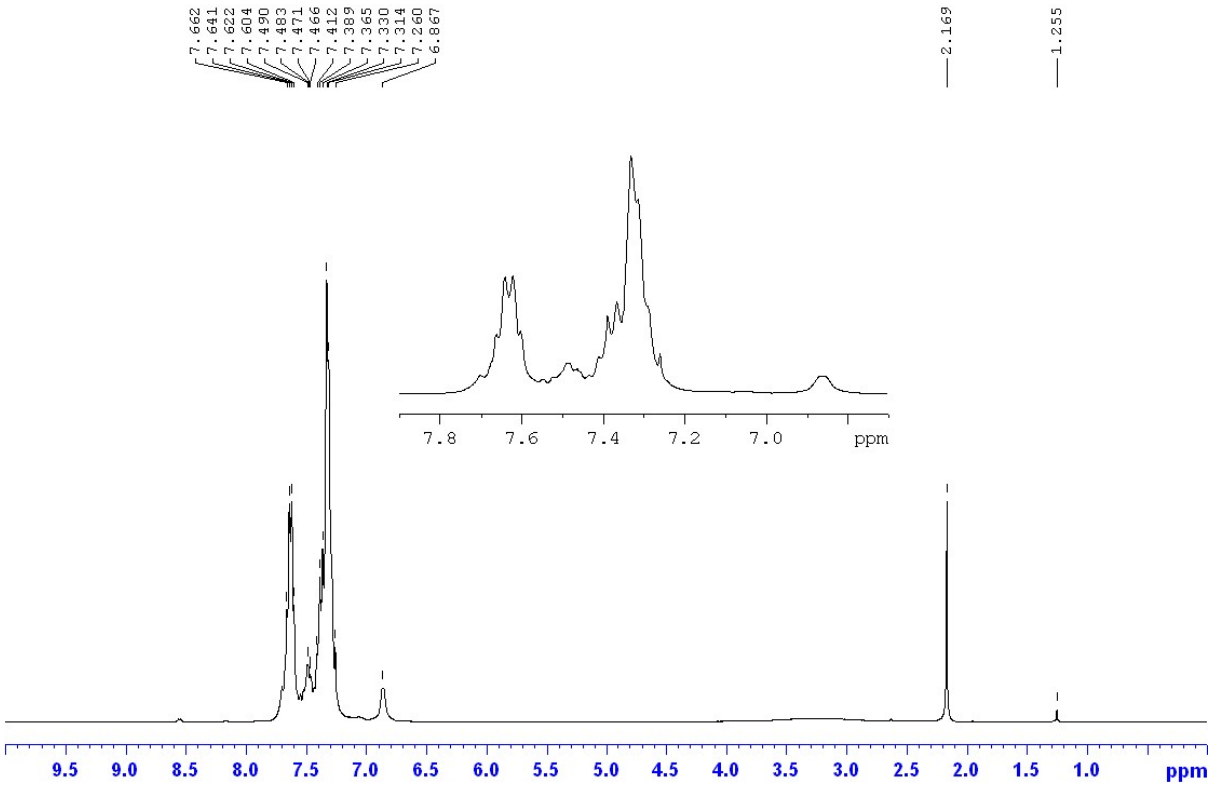

Fig. S1 ^{1}H NMR (300 MHz, $CDCl_3$) of $[PdCl(PPh_3)_2(4\text{-Spy})]$ (**1a**).

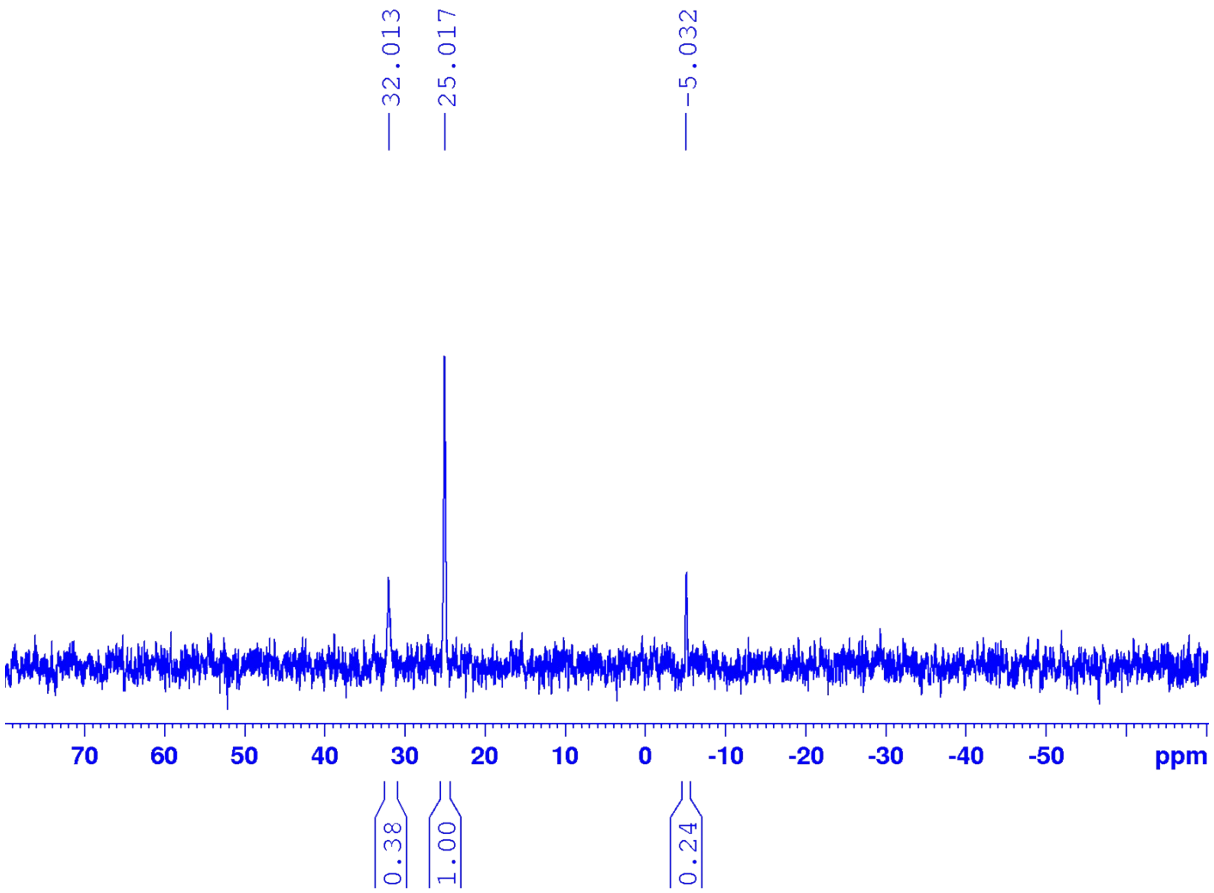

Fig. S2 $^{31}P\{^{1}H\}$ NMR (121.5 MHz, $CDCl_3$) of $[PdCl(PPh_3)_2(4\text{-Spy})]$ (**1a**).

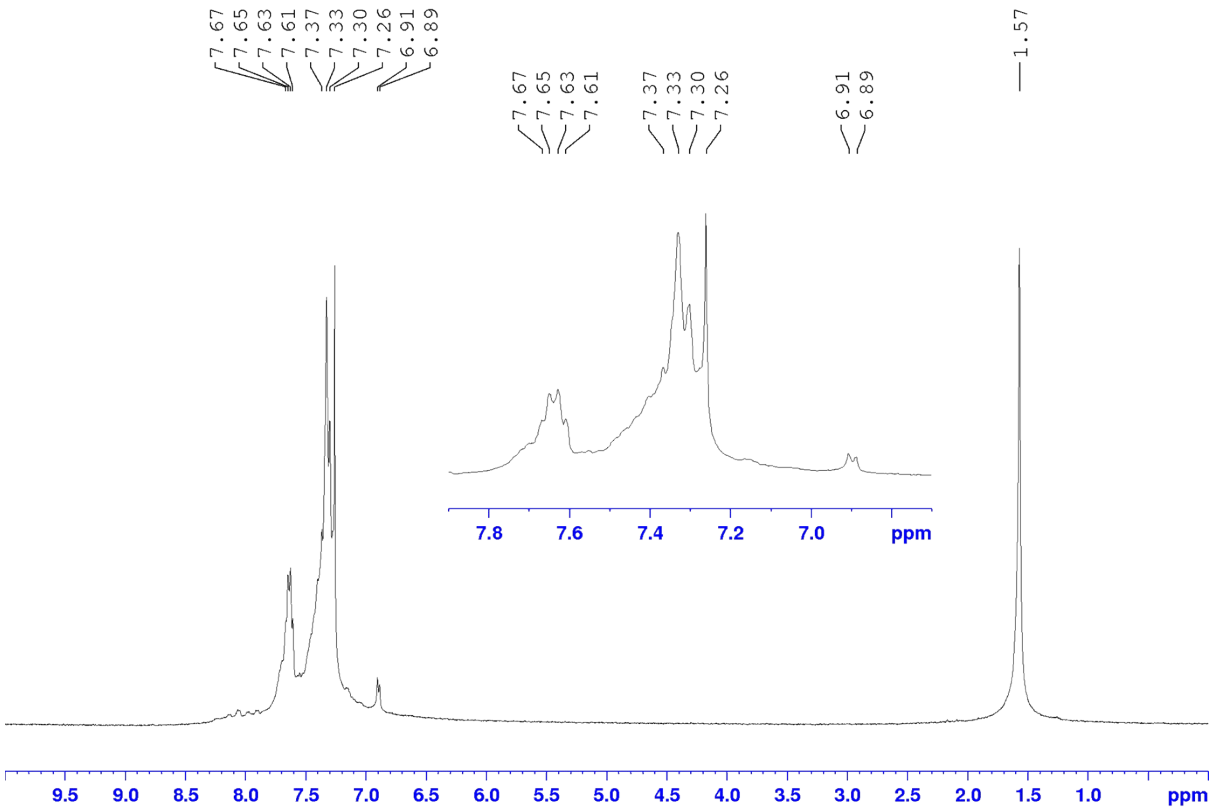

Fig. S3 ^{1}H NMR (300 MHz, $CDCl_3$) of $[PdCl(PPh_3)_2(4\text{-Sepy})]$ (**1b**).

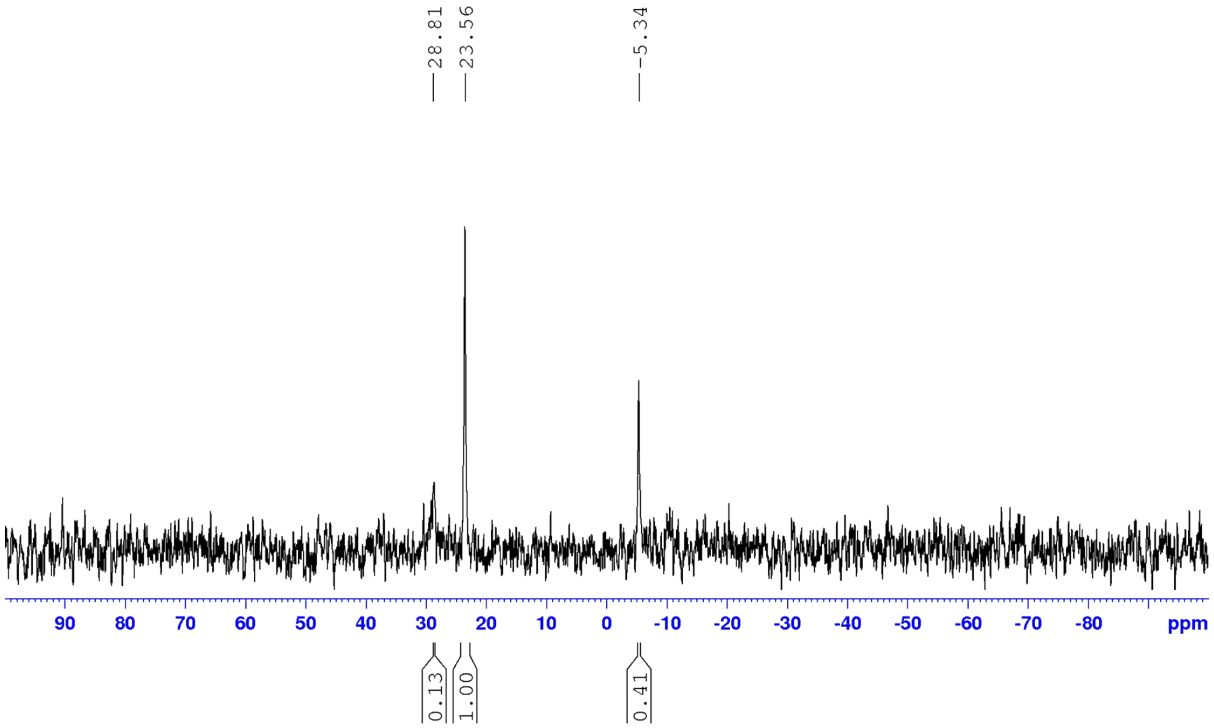

Fig. S4 $^{31}P\{^{1}H\}$ NMR (121.5 MHz, $CDCl_3$) of $[PdCl(PPh_3)_2(4\text{-Sepy})]$ (**1b**).

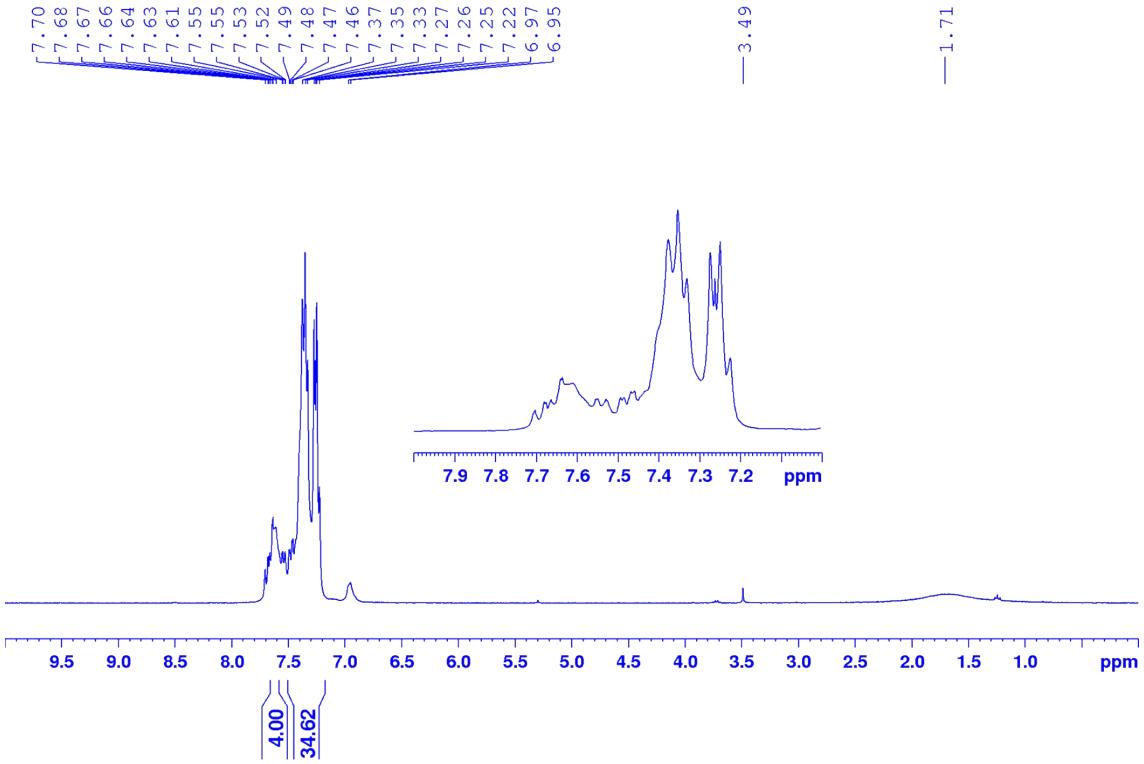

Fig. S5 ^{1}H NMR (300 MHz, $CDCl_3$) of $[\{Pd(PPh_3)_2(4\text{-Spy})_2\}\{Cu(PPh_3)_2Cl\}_2]$ (**3**) prepared from route (i).

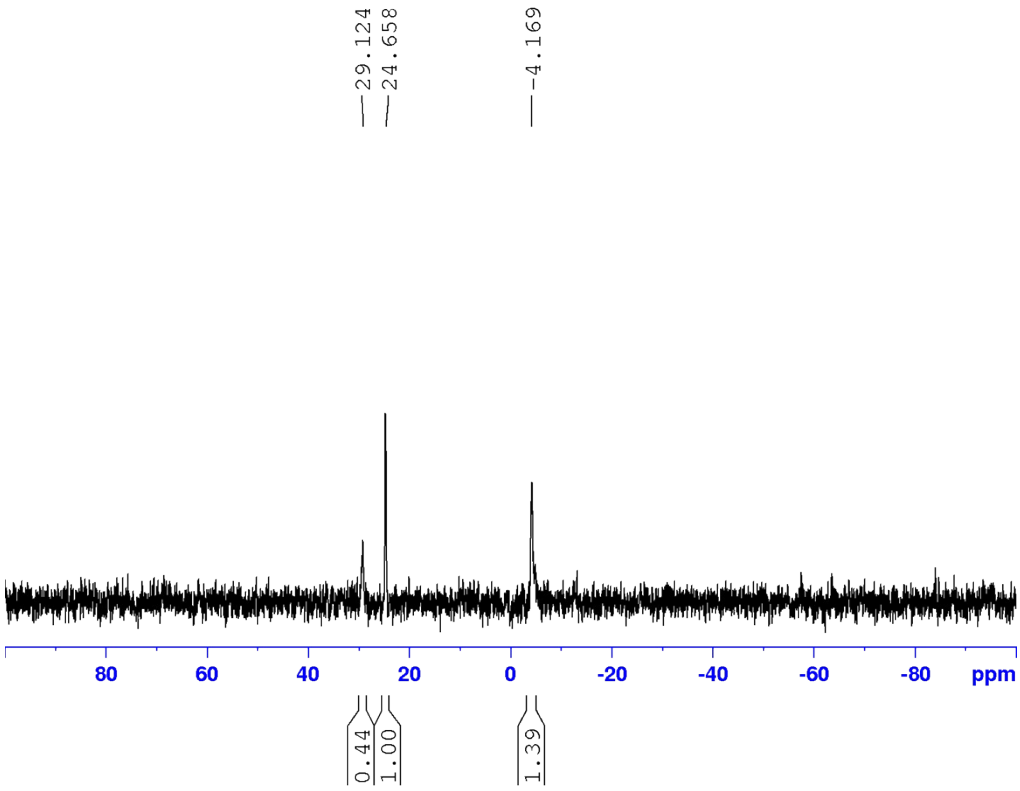

Fig. S6 $^{31}P\{^{1}H\}$ NMR (121.5 MHz, $CDCl_3$) of $[\{Pd(PPh_3)_2(4\text{-}Spy)_2\}\{Cu(PPh_3)_2Cl\}_2]$ (**3**) prepared from route (i).

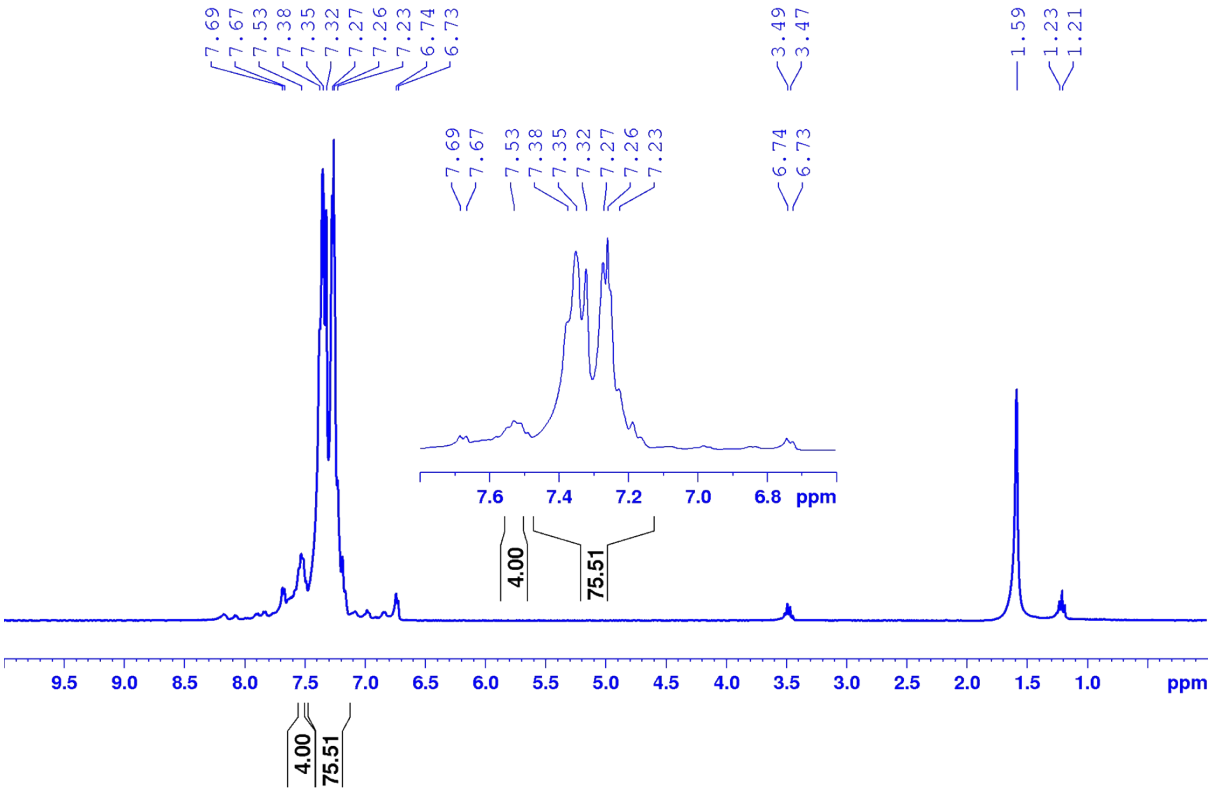

Fig. S7 ^{1}H NMR (300 MHz, $CDCl_3$) of $[\{Pd(PPh_3)_2(4\text{-}Spy)_2\}\{Cu(PPh_3)_2Cl\}_2]$ (**3**) prepared from route (ii).

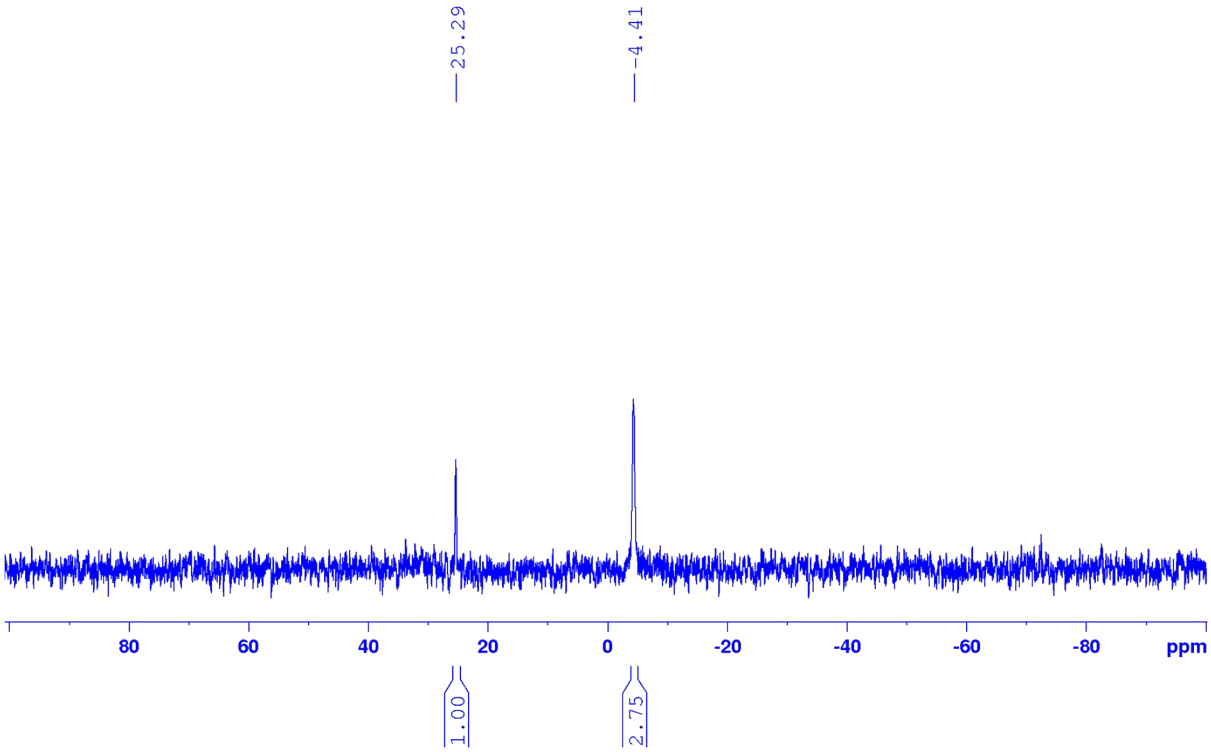

Fig. S8 $^{31}P\{^{1}H\}$ NMR (121.5 MHz, $CDCl_3$) of $[\{Pd(PPh_3)_2(4\text{-}Spy)_2\}\{Cu(PPh_3)_2Cl\}_2]$ (**3**) prepared from route (ii).

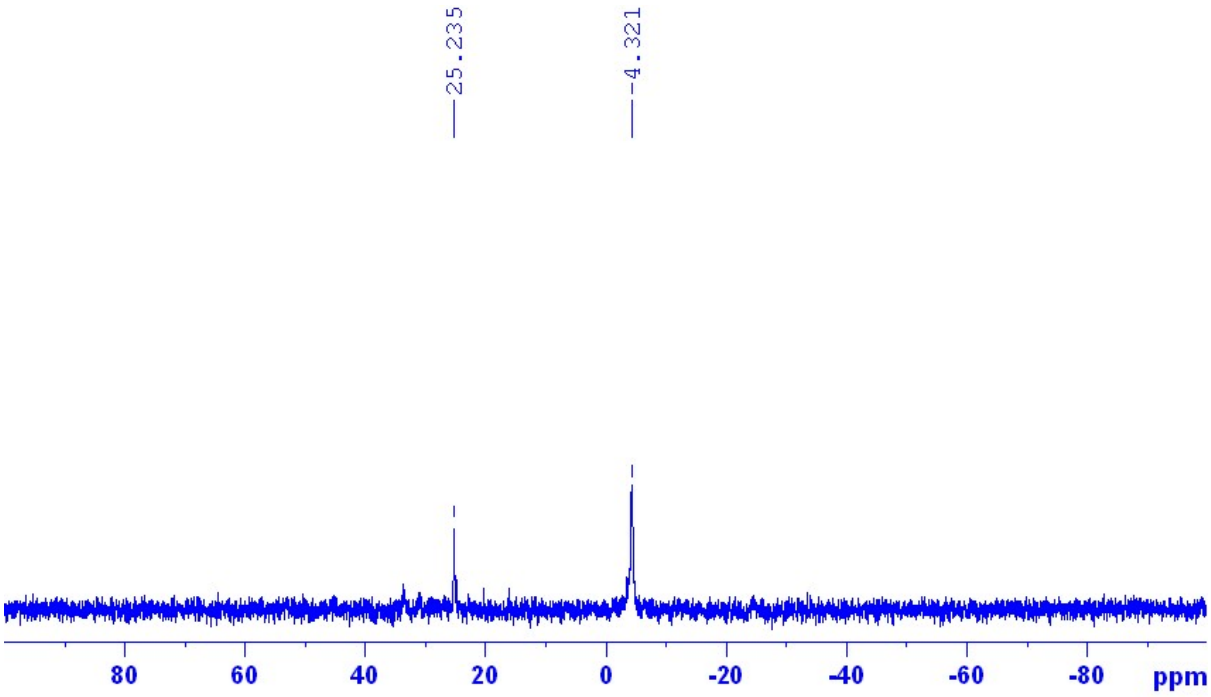

Fig. S9 $^{31}P\{^{1}H\}$ NMR (121.5 MHz, $CDCl_3$) of $[\{Pd(PPh_3)_2(4\text{-}Spy)_2\}\{Cu(PPh_3)_2Cl\}_2]$ (**3**) prepared from route (ii) after 1 day.

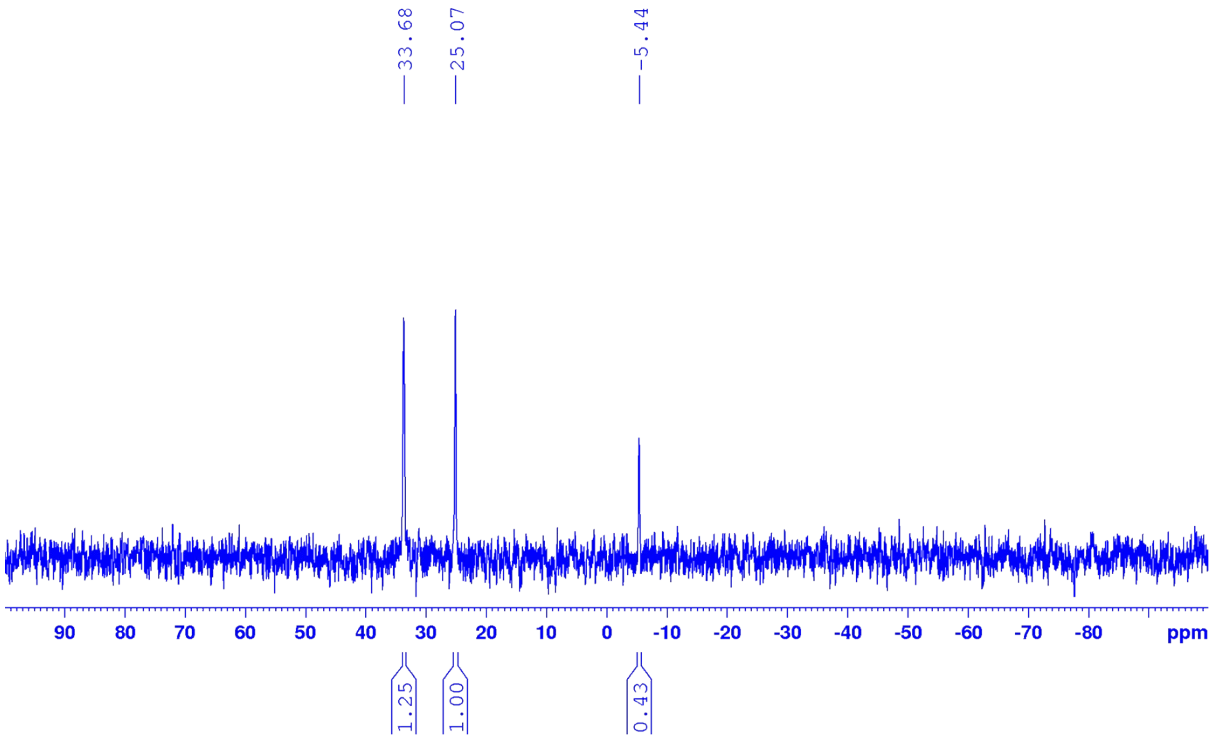

Fig. S10 $^{31}P\{^{1}H\}$ NMR (121.5 MHz, $CDCl_3$) of $[Pd(PPh_3)_2(4\text{-}Spy)_2]$ (**2a**).

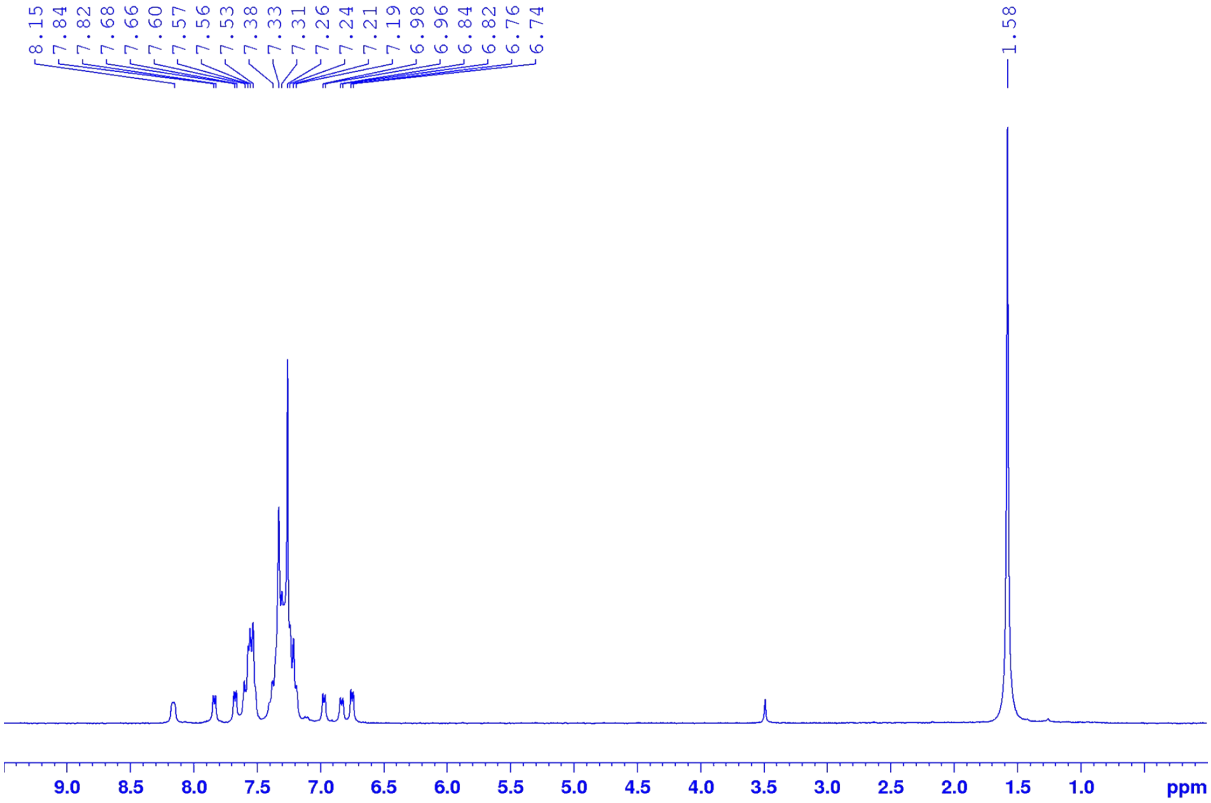

Fig. S11 ^{1}H NMR (300 MHz, $CDCl_3$) of $[Pd(PPh_3)_2(4\text{-}Spy)_2]$ (**2a**).

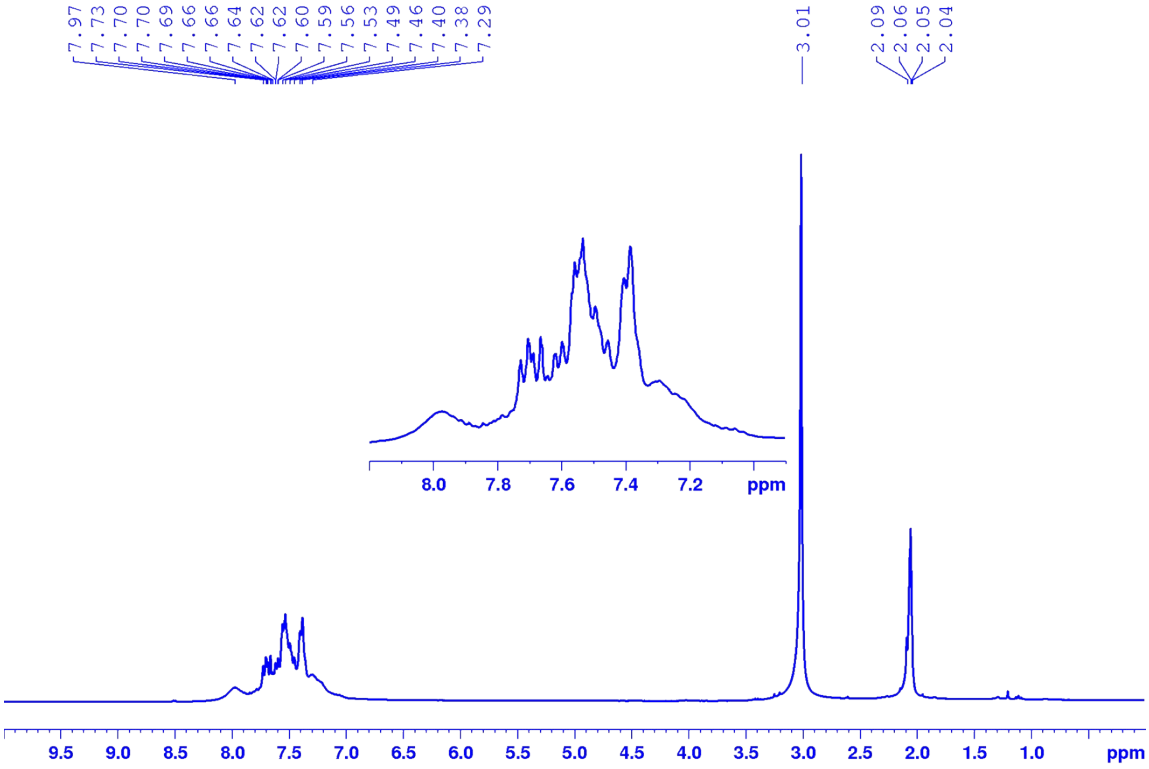

Fig. S12 ^{1}H NMR (300 MHz, Acetone-d_6) of $[Pd(PPh_3)_2(4\text{-}Sepy)_2]$ (**2b**).

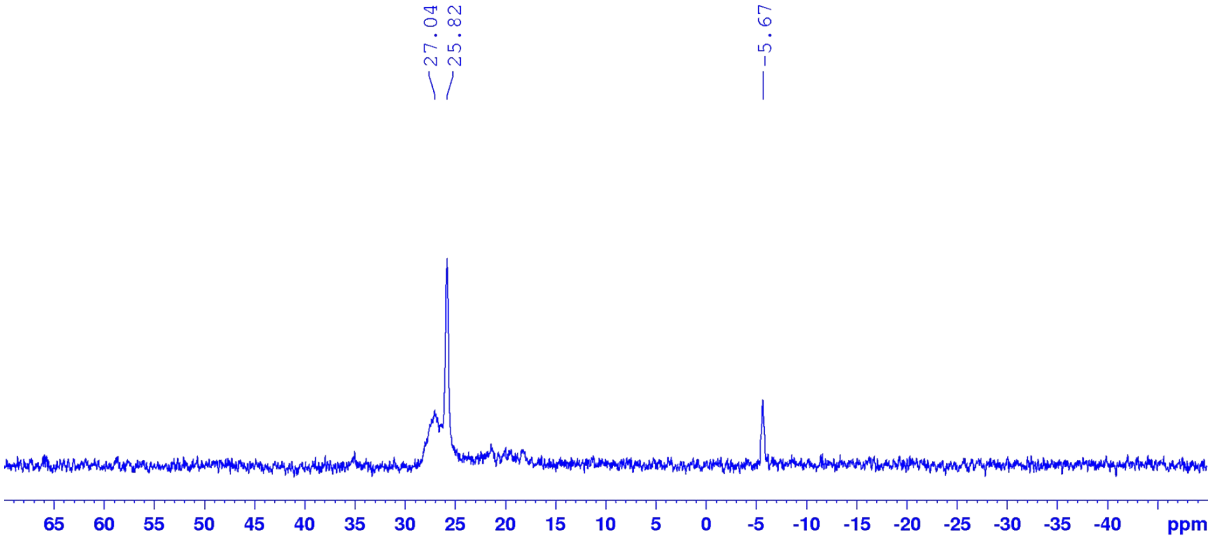

Fig. S13 $^{31}P\{^{1}H\}$ NMR (121.5 MHz, Acetone-d_6) of $[Pd(PPh_3)_2(4\text{-Sepy})_2]$ (**2b**).

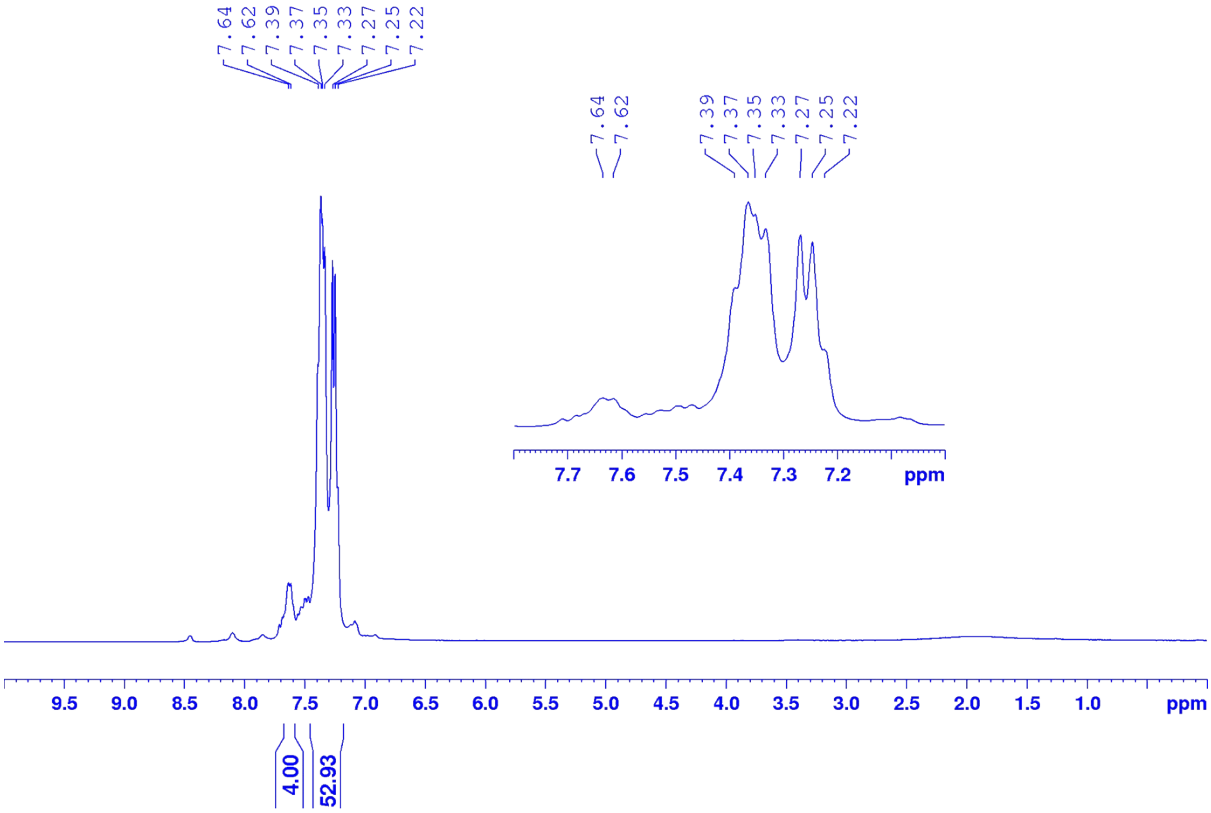

Fig. S14 ^{1}H NMR (300 MHz, $CDCl_3$) of $[\{Pd(PPh_3)_2(4\text{-Sepy})_2\}\{Cu(PPh_3)_2Cl\}_2]$ (**4**) prepared from route (i).

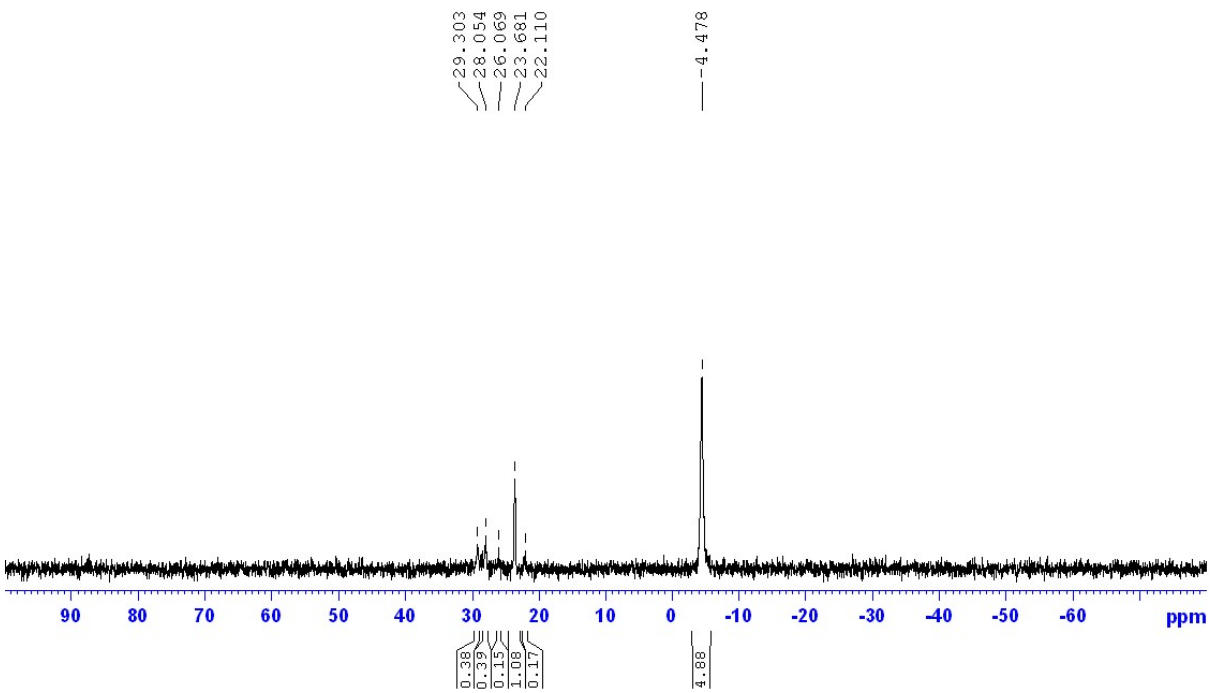

Fig. S15 $^{31}P\{^{1}H\}$ NMR (121.5 MHz, $CDCl_3$) of $[\{Pd(PPh_3)_2(4\text{-Sepy})_2\}\{Cu(PPh_3)_2Cl\}_2]$ (**4**) prepared from route (i).

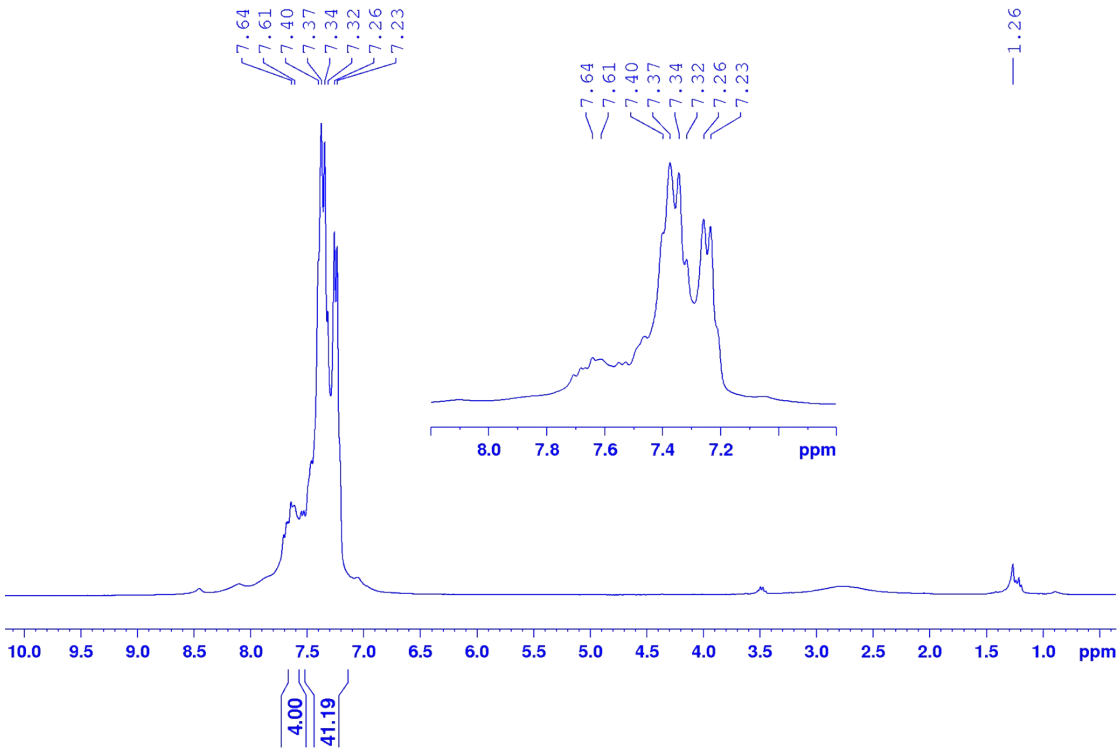

Fig. S16 ^{1}H NMR (300 MHz, $CDCl_3$) of $[\{Pd(PPh_3)_2(4\text{-Sepy})_2\}\{Cu(PPh_3)_2Cl\}_2]$ (**4**) prepared from route (ii).

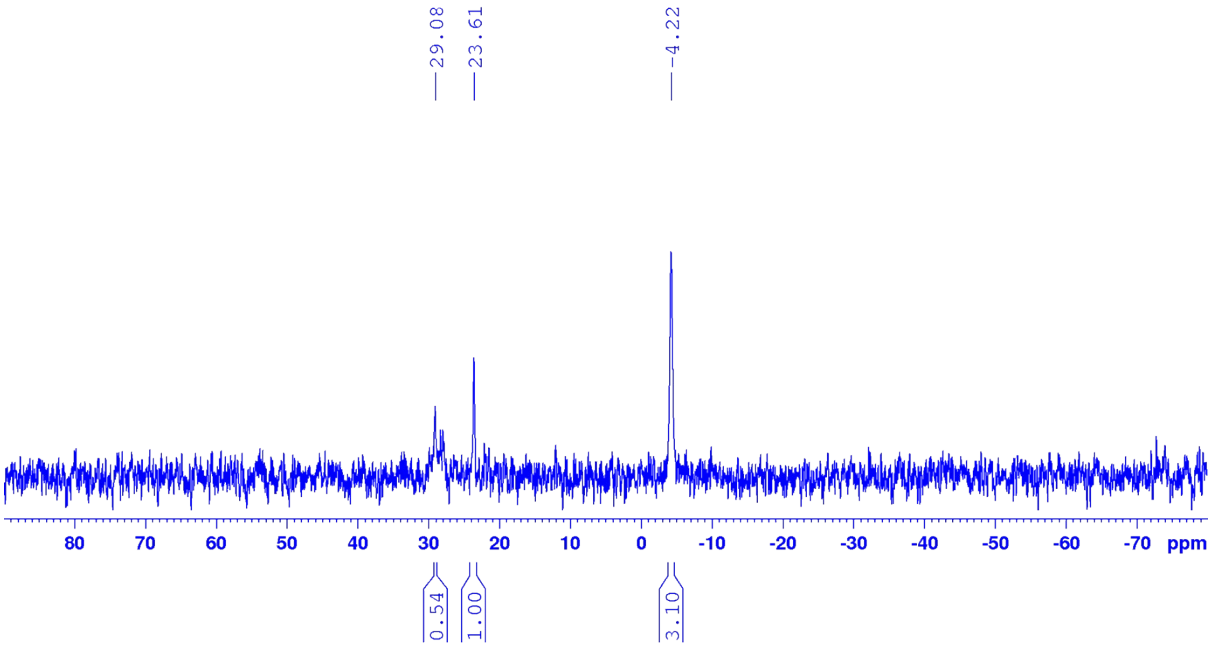

Fig. S17 $^{31}P\{^{1}H\}$ NMR (121.5 MHz, $CDCl_3$) of $[\{Pd(PPh_3)_2(4\text{-Sepy})_2\}\{Cu(PPh_3)_2Cl\}_2]$ (**4**) prepared from route (ii).

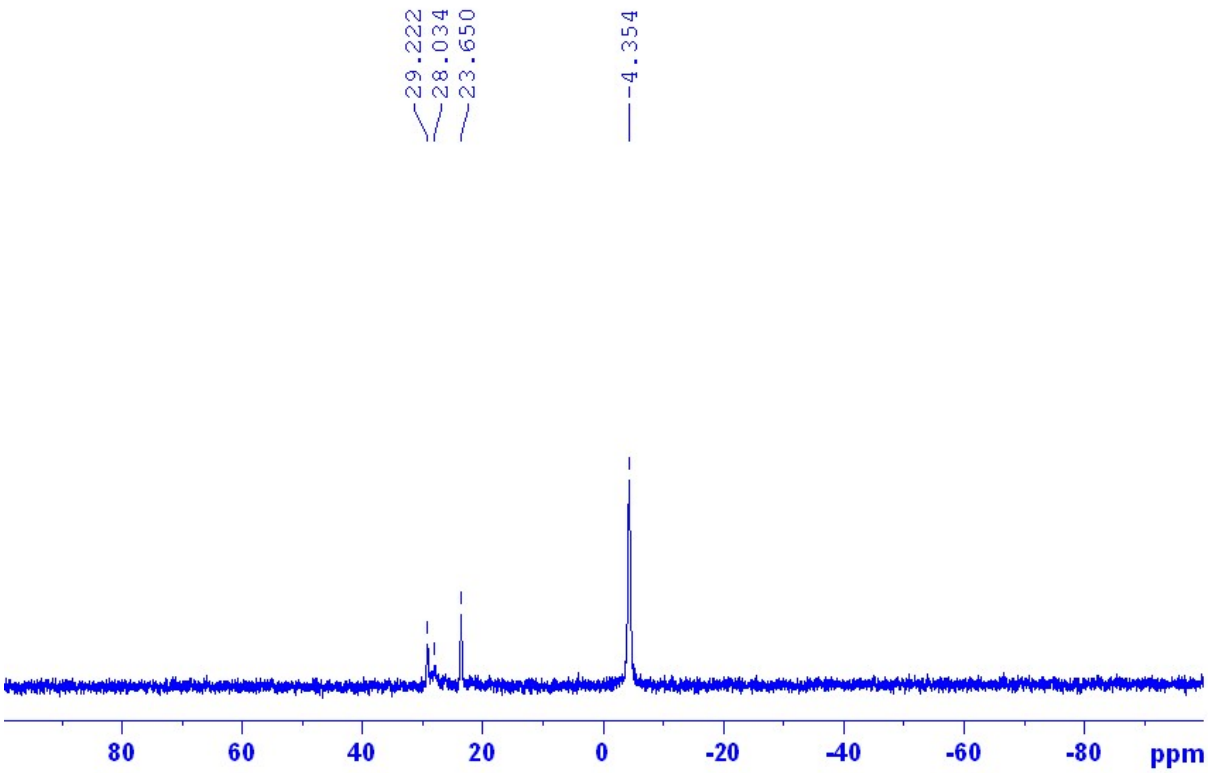

Fig. S18 $^{31}P\{^{1}H\}$ NMR (121.5 MHz, $CDCl_3$) of $[\{Pd(PPh_3)_2(4\text{-Sepy})_2\}\{Cu(PPh_3)_2Cl\}_2]$ (**4**) prepared from route (ii) after 1 day.

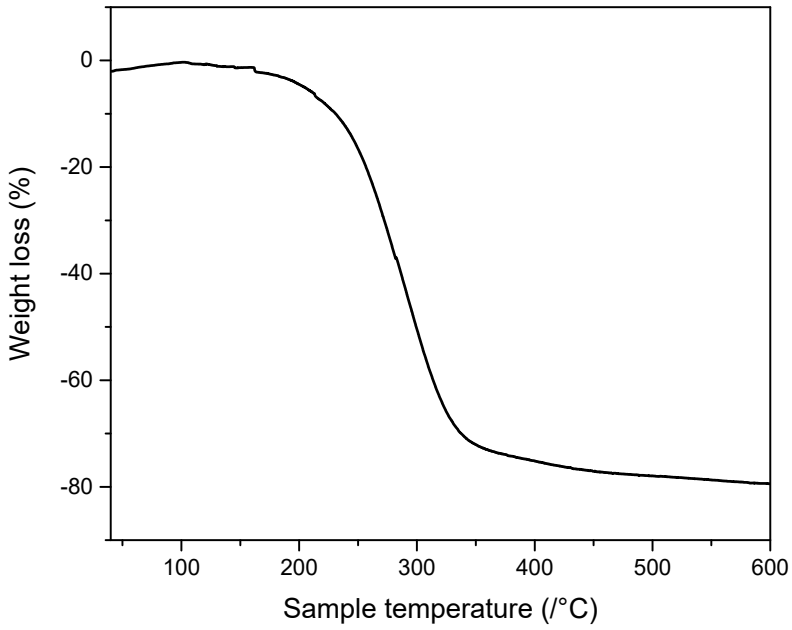

Fig. S19 Thermogravimetric curve of $[\{Pd(PPh_3)_2(4\text{-}Sepy)_2\}\{Cu(PPh_3)_2Cl\}_2]$ (**4**).

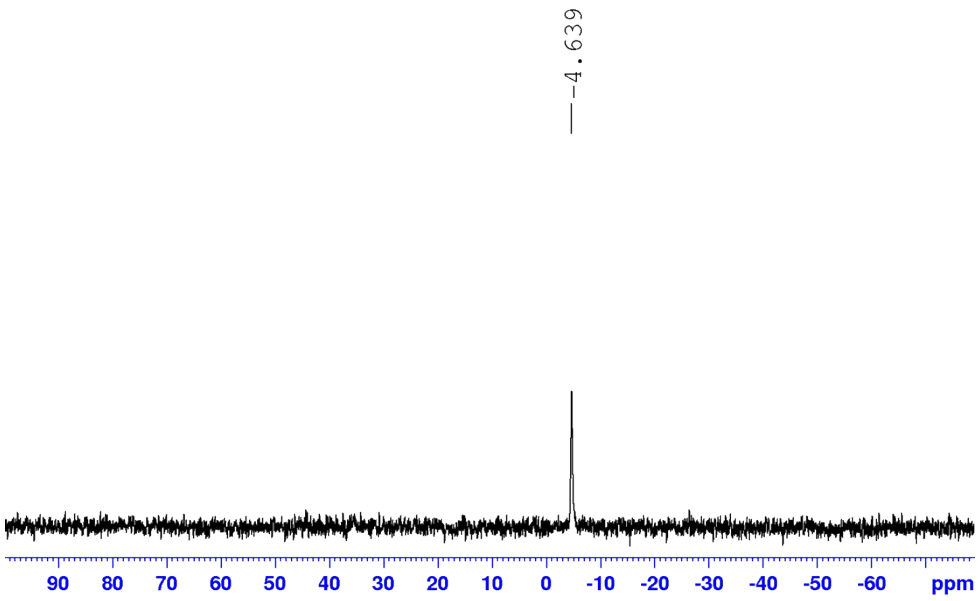

Fig. S20 $^{31}P\{^{1}H\}$ NMR (300 MHz, $CDCl_3$) of $[Cu(PPh_3)_3Cl]$.

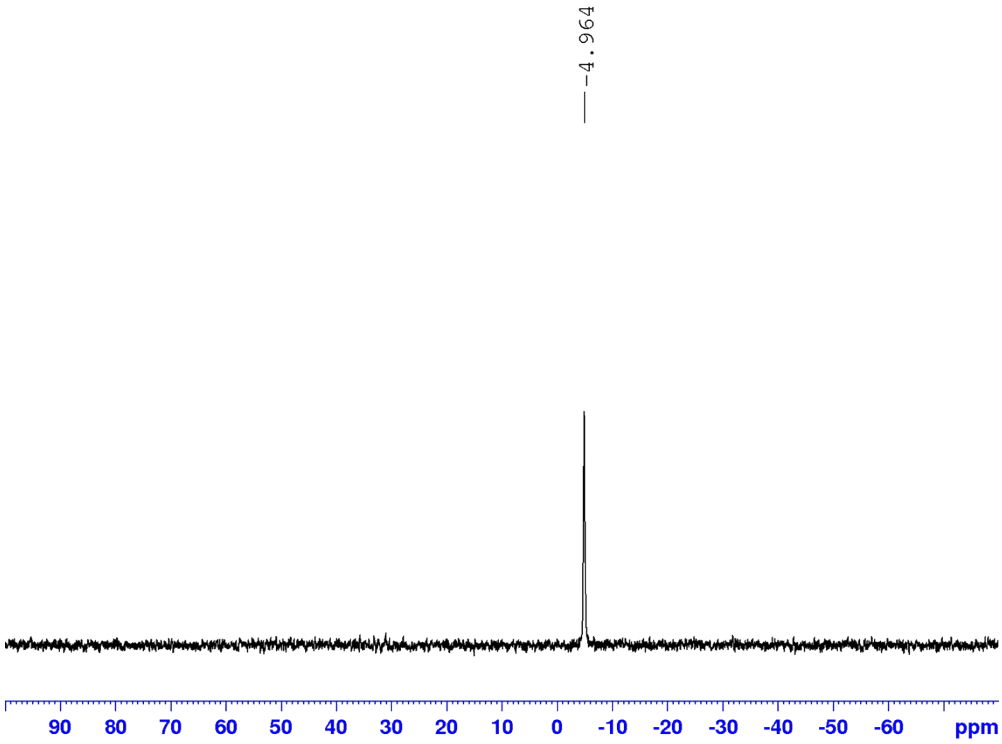

Fig. S21 $^{31}P\{^{1}H\}$ NMR (300 MHz, $CDCl_3$) of $[Cu(PPh_3)_3Cl]$ + PPh_3 in (1:1 stoichiometry) immediately.

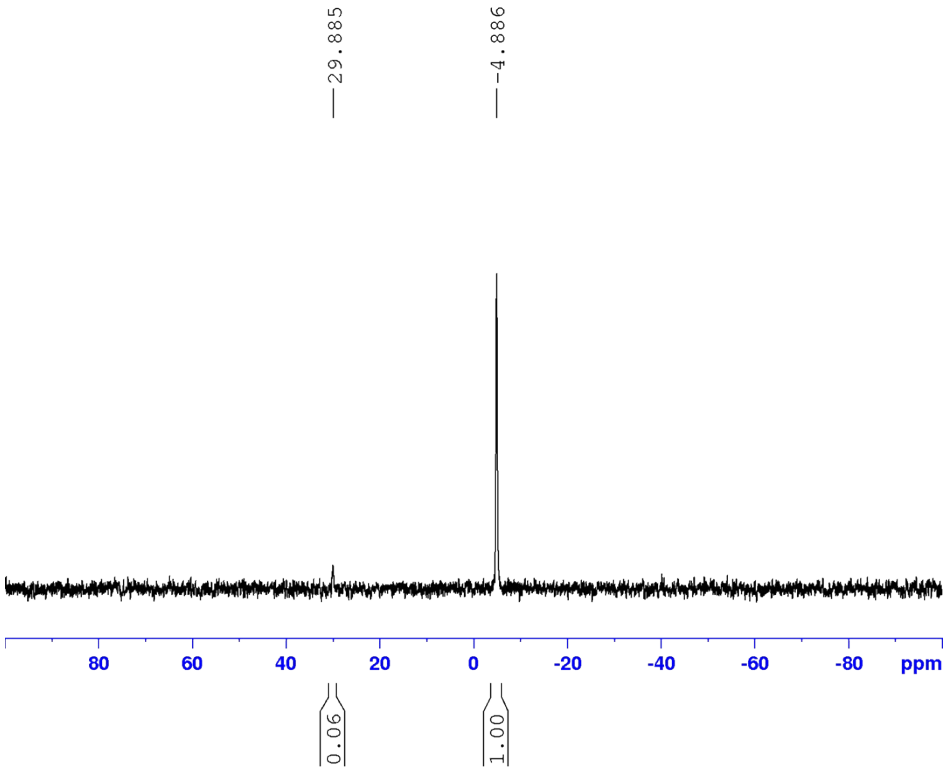

Fig. S22 $^{31}P\{^{1}H\}$ NMR (300 MHz, $CDCl_3$) of $[Cu(PPh_3)_3Cl]$ + PPh_3 in (1:1 stoichiometry) after 1day.

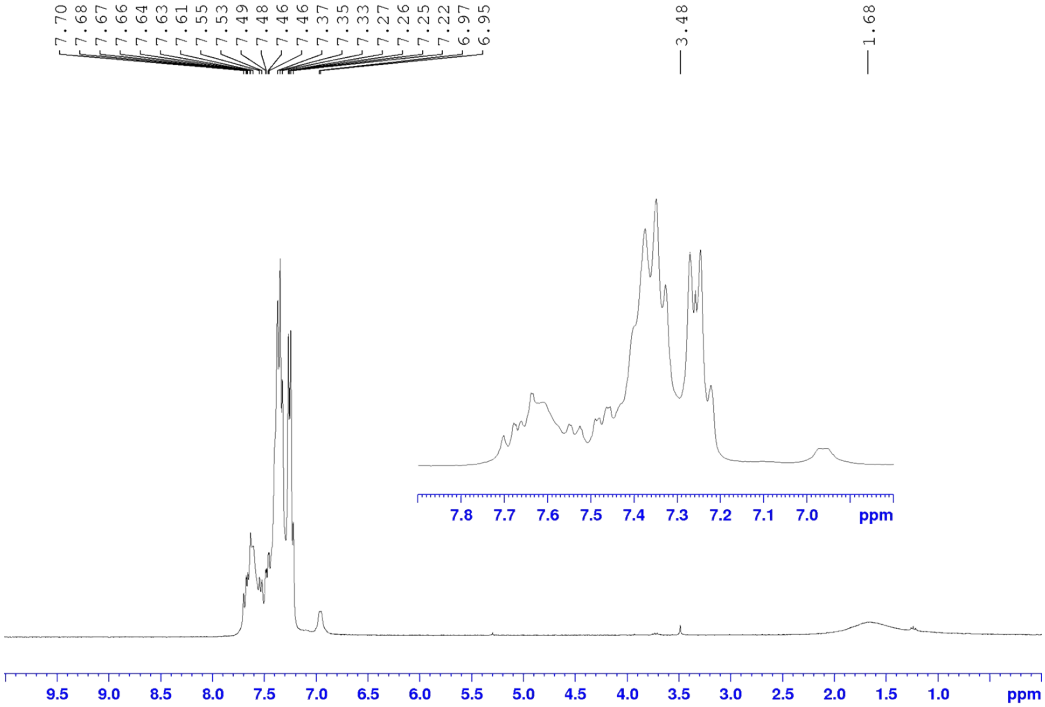

Fig. S23 ^{1}H NMR (300 MHz, $CDCl_3$) of [{$Pd(PPh_3)_2$(4-Spy)$_2$}{$Cu(PPh_3)_2Cl$}$_2$] (**3**) prepared from route (i) after overnight.

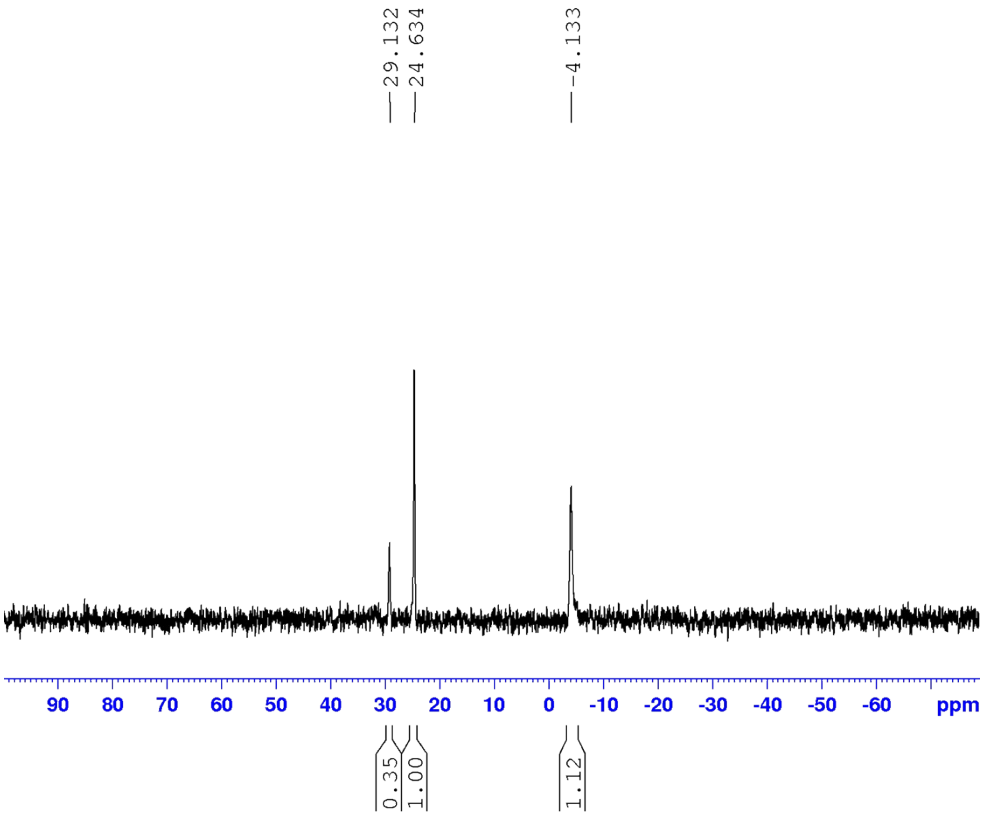

Fig. S24 ^{31}P{^{1}H} NMR (121.5 MHz, $CDCl_3$) of [{$Pd(PPh_3)_2$(4-Spy)$_2$}{$Cu(PPh_3)_2Cl$}$_2$] (**3**) prepared from route (i) after overnight.

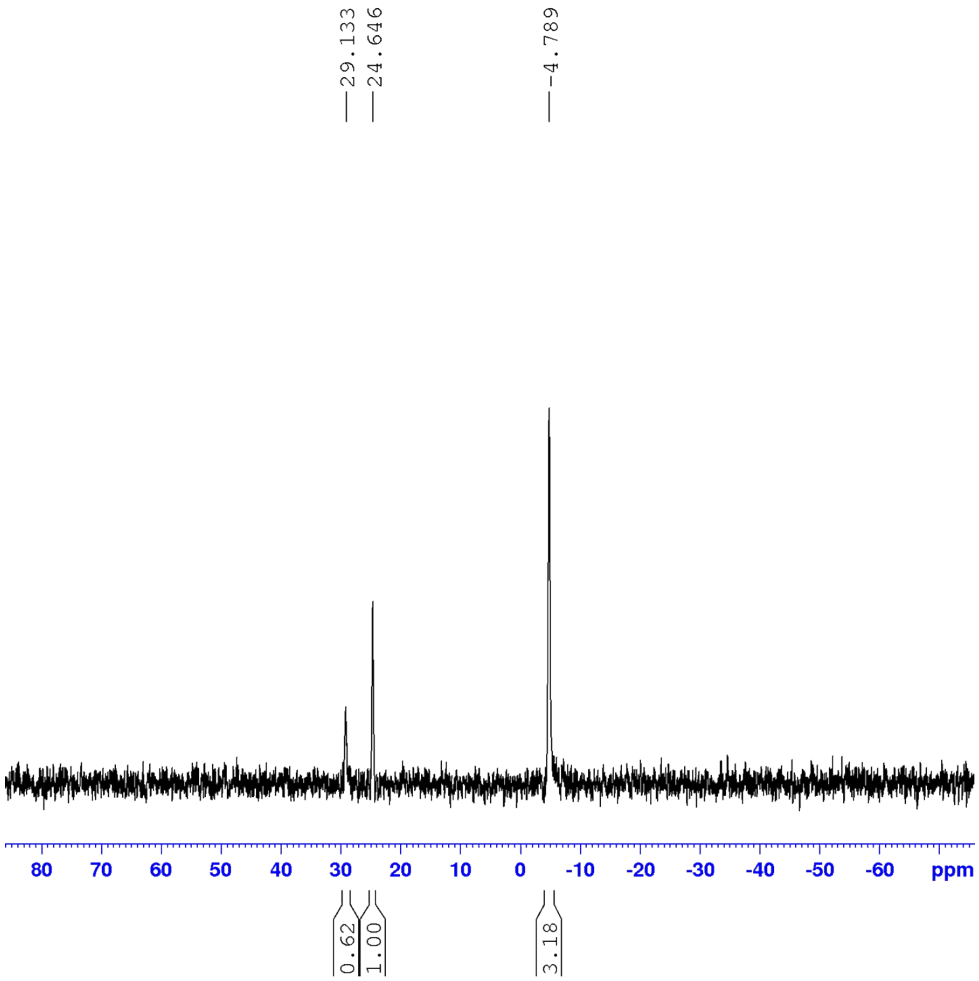

Fig. S25 $^{31}P\{^{1}H\}$ NMR (121.5 MHz, $CDCl_3$) of $[\{Pd(PPh_3)_2(4\text{-}Spy)_2\}\{Cu(PPh_3)_2Cl\}_2]$ (**3**) prepared from route (i) + PPh_3 in (1:2 stoichiometry) immediately.

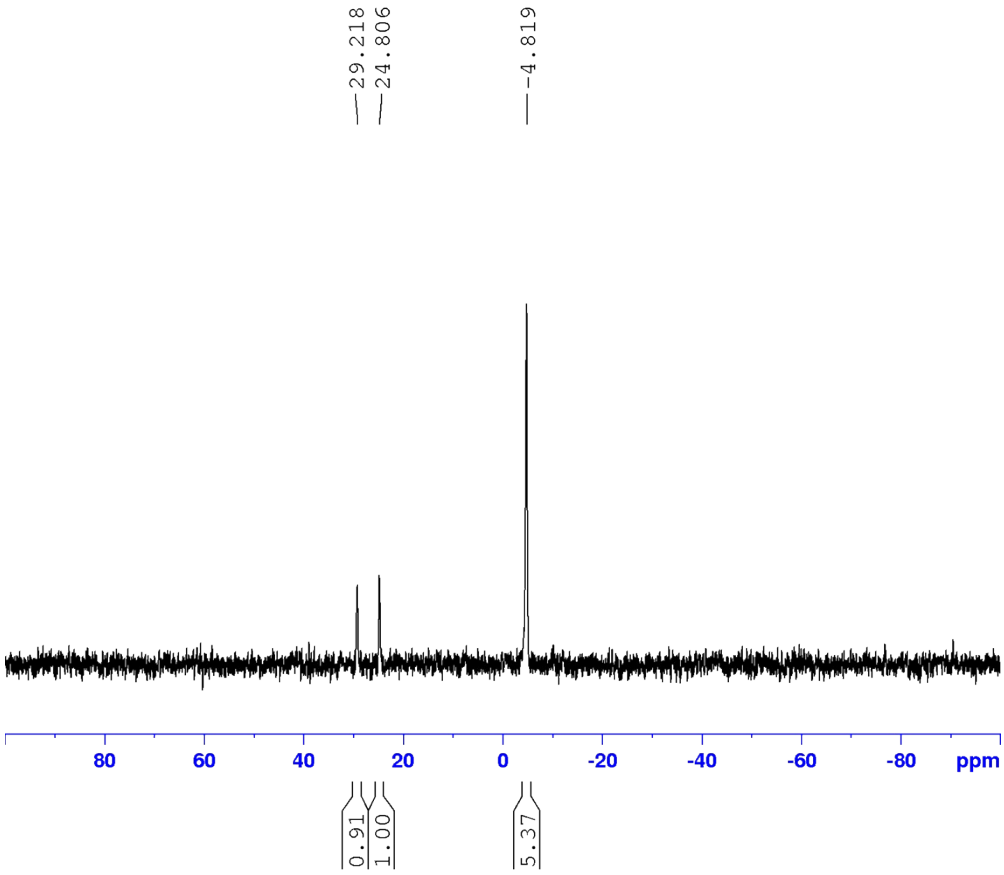

Fig. S26 $^{31}P\{^{1}H\}$ NMR (121.5 MHz, $CDCl_3$) of $[\{Pd(PPh_3)_2(4\text{-}Spy)_2\}\{Cu(PPh_3)_2Cl\}_2]$ (**3**) prepared from route (i) + PPh_3 in (1:2 stoichiometry) after 2 days.

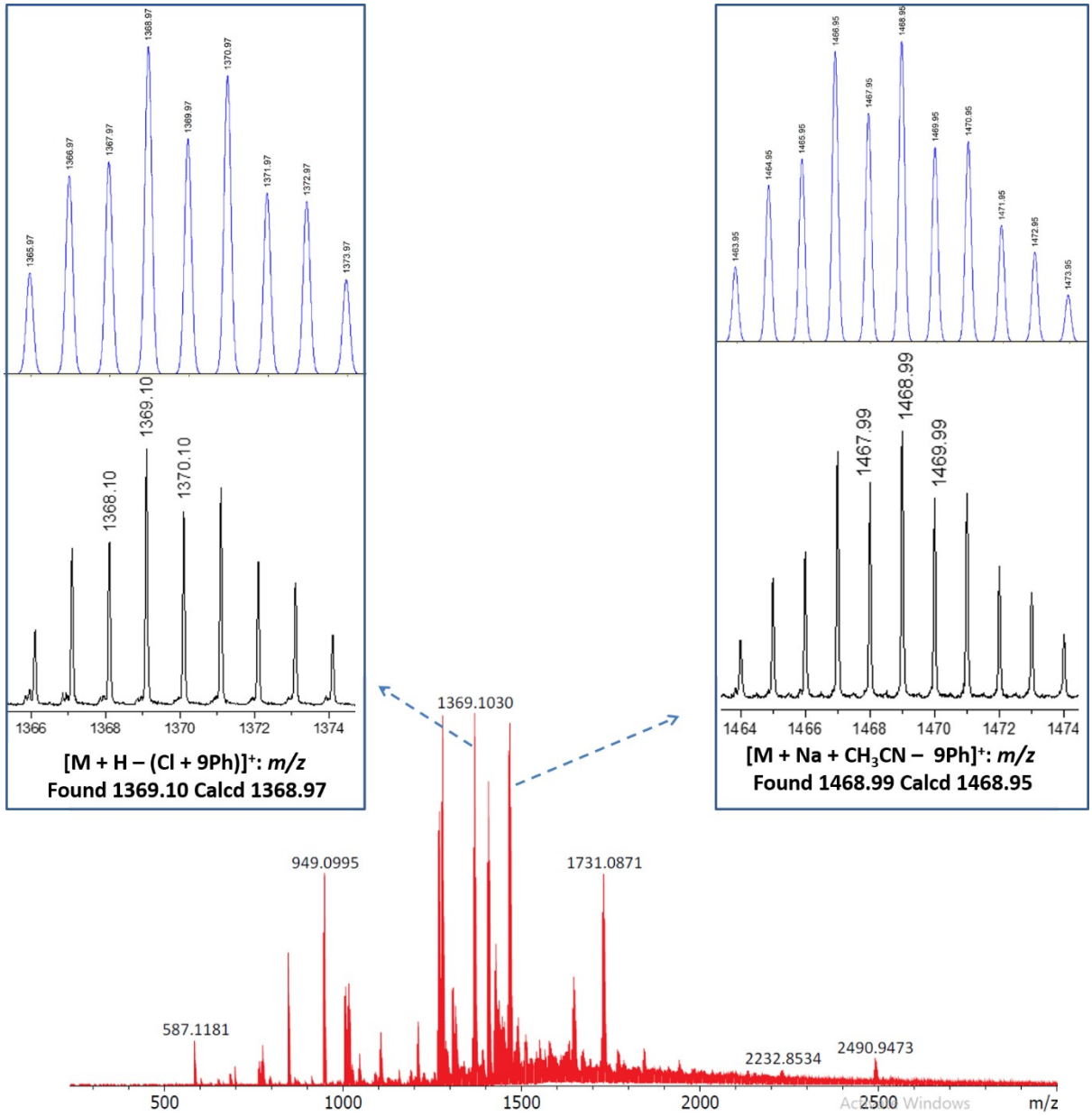

Fig. S27 ESI-mass spectrum of $[\{Pd(PPh_3)_2(4\text{-}Spy)_2\}\{Cu(PPh_3)_2Cl\}_2]$ (**3**). The insets show the experimentally obtained (below) isotope patterns of the fragments with those simulated (above) on the basis of natural isotope abundances. The found and calcd values are for the most abundant peak of ion.

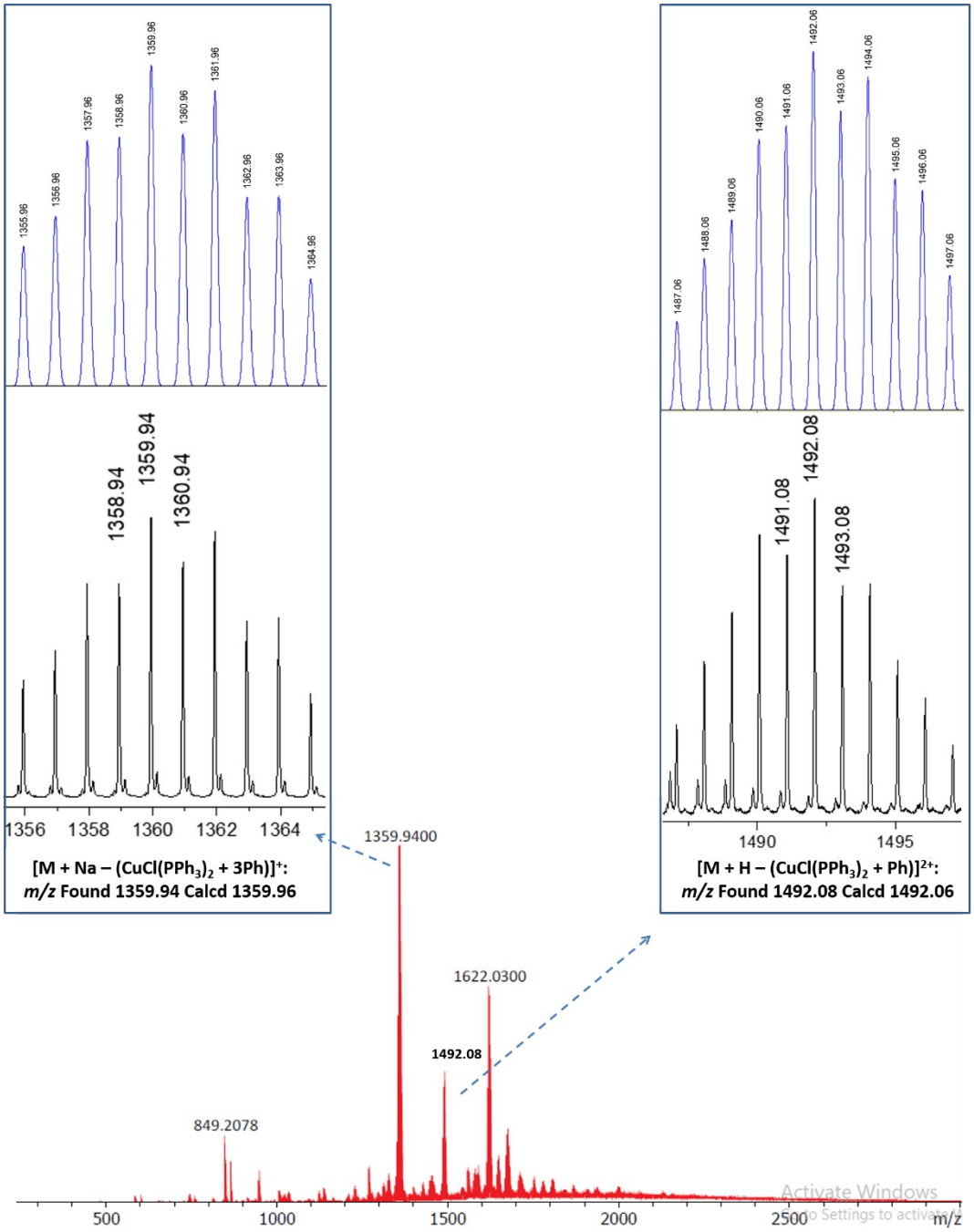

Fig. S28 ESI-mass spectrum of $[\{Pd(PPh_3)_2(4\text{-Sepy})_2\}\{Cu(PPh_3)_2Cl\}_2]$ (**4**). The insets show the experimentally obtained (below) isotope patterns of the fragments with those simulated (above) on the basis of natural isotope abundances. The found and calcd values are for the most abundant peak of ion.

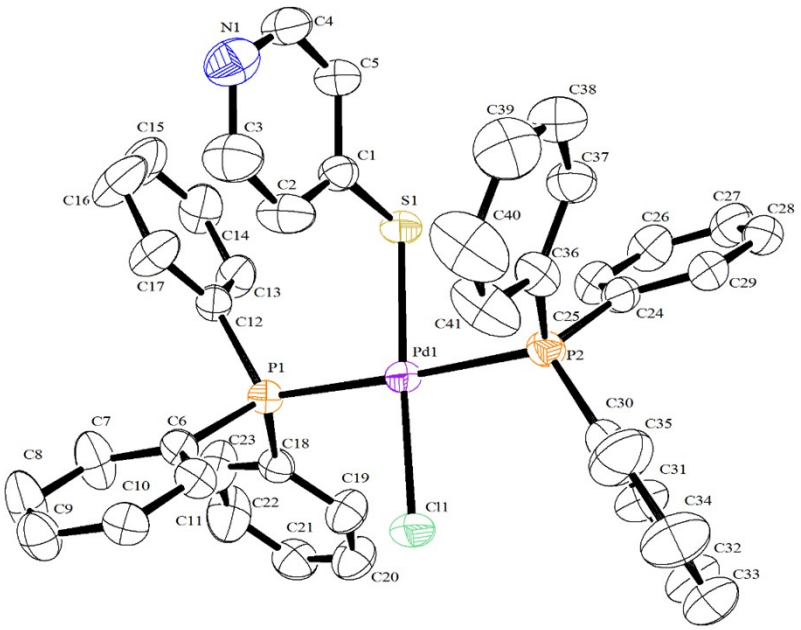

Fig. S29 ORTEP diagram of [PdCl(4-Spy)(PPh_3)$_2$] (**1a**) ellipsoids drawn at 50% probability. The hydrogen atoms are omitted for clarity.

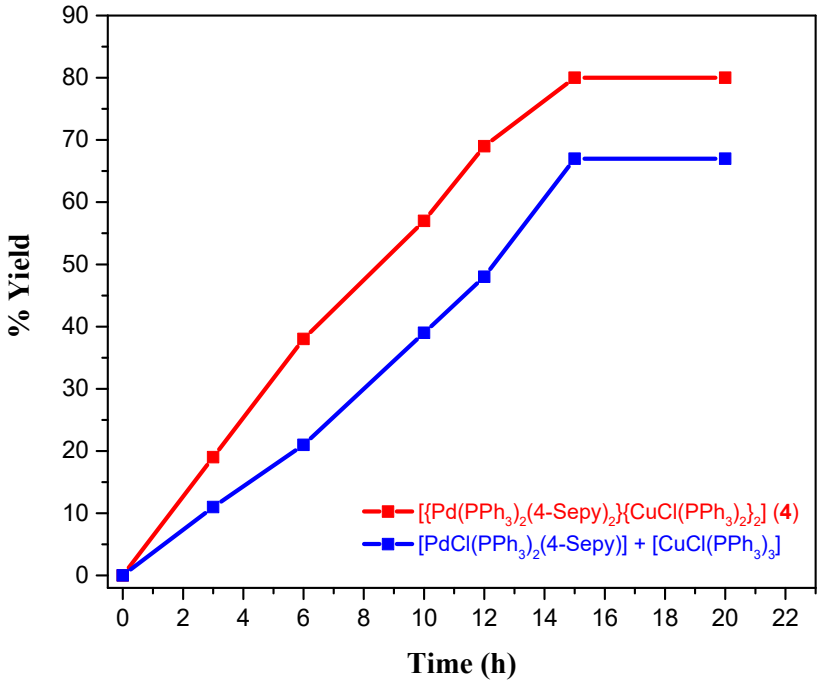

Fig. S30 Kinetic study of catalysis reaction using catalysts [{$Pd(PPh_3)_2$(4-Sepy)$_2$}{$Cu(PPh_3)_2Cl$}$_2$] (**4**) and mixture of **1b** with [$CuCl(PPh_3)_3$].

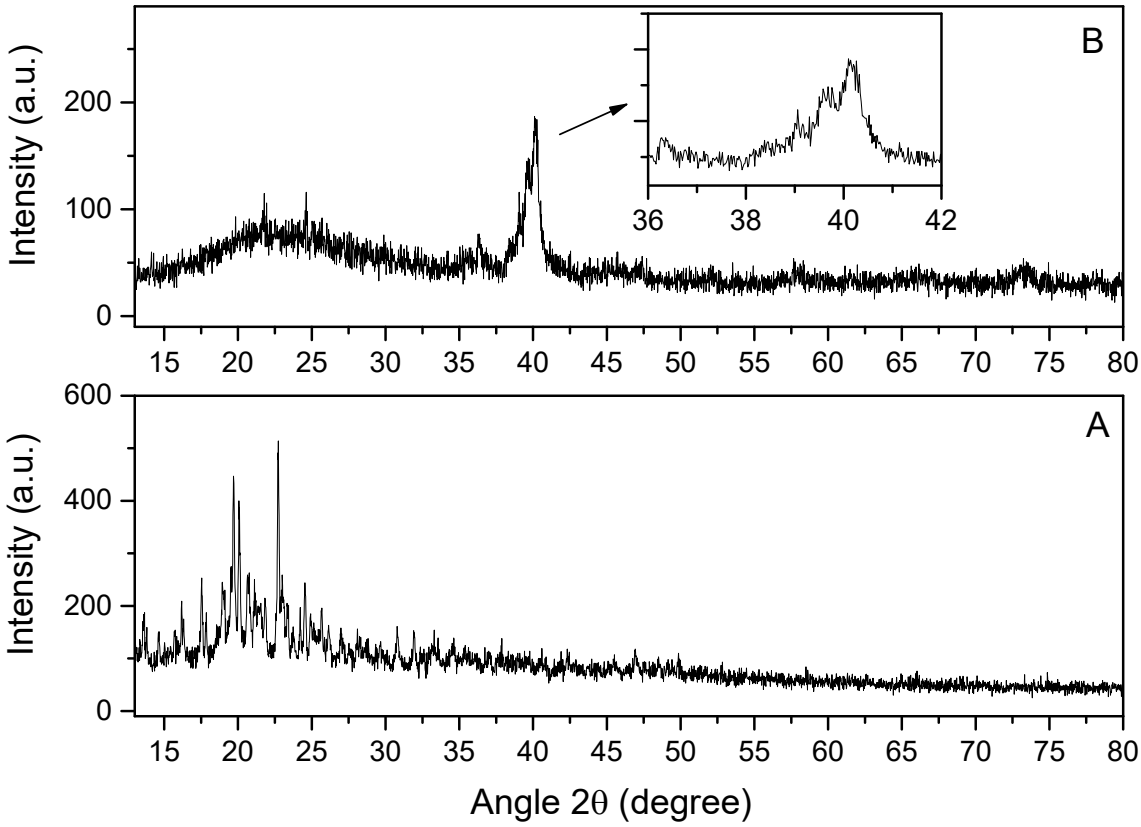

Fig. S31 Powder XRD pattern of (A) $[\{Pd(PPh_3)_2(4\text{-}Sepy)_2\}\{Cu(PPh_3)_2Cl\}_2]$ (**4**) before catalysis experiment and (B) black residue obtained after catalysis experiment.

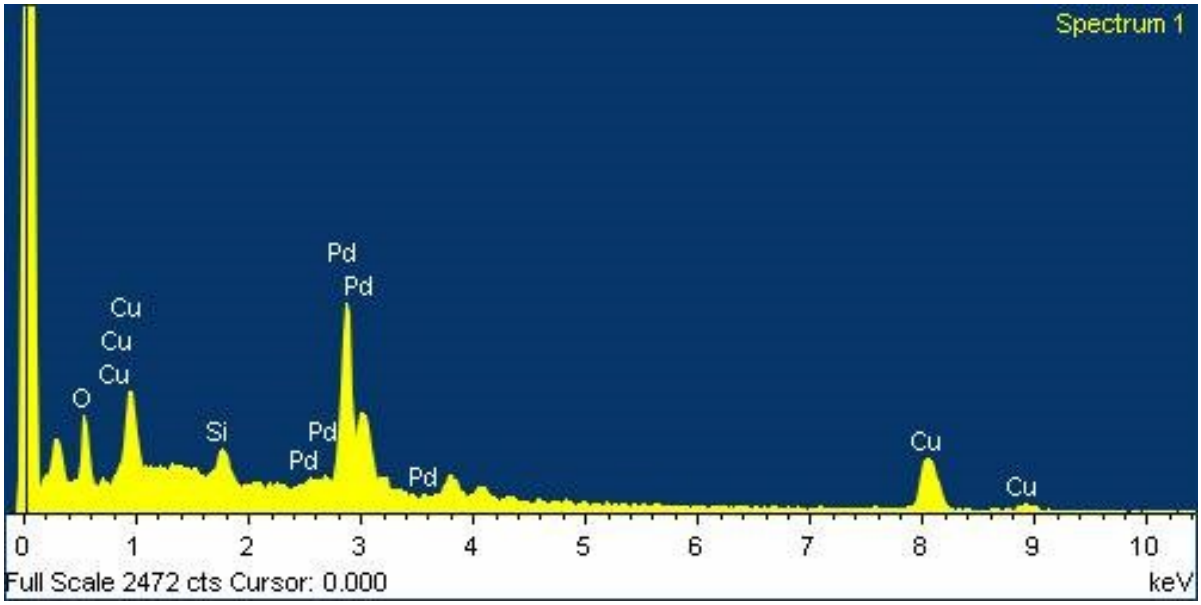

Fig. S32 Energy Dispersive X-ray Analysis (EDAX) spectrum of the black residue obtained after catalysis experiment of [{$Pd(PPh_3)_2(4\text{-}Sepy)_2$}{$Cu(PPh_3)_2Cl$}$_2$] (**4**).

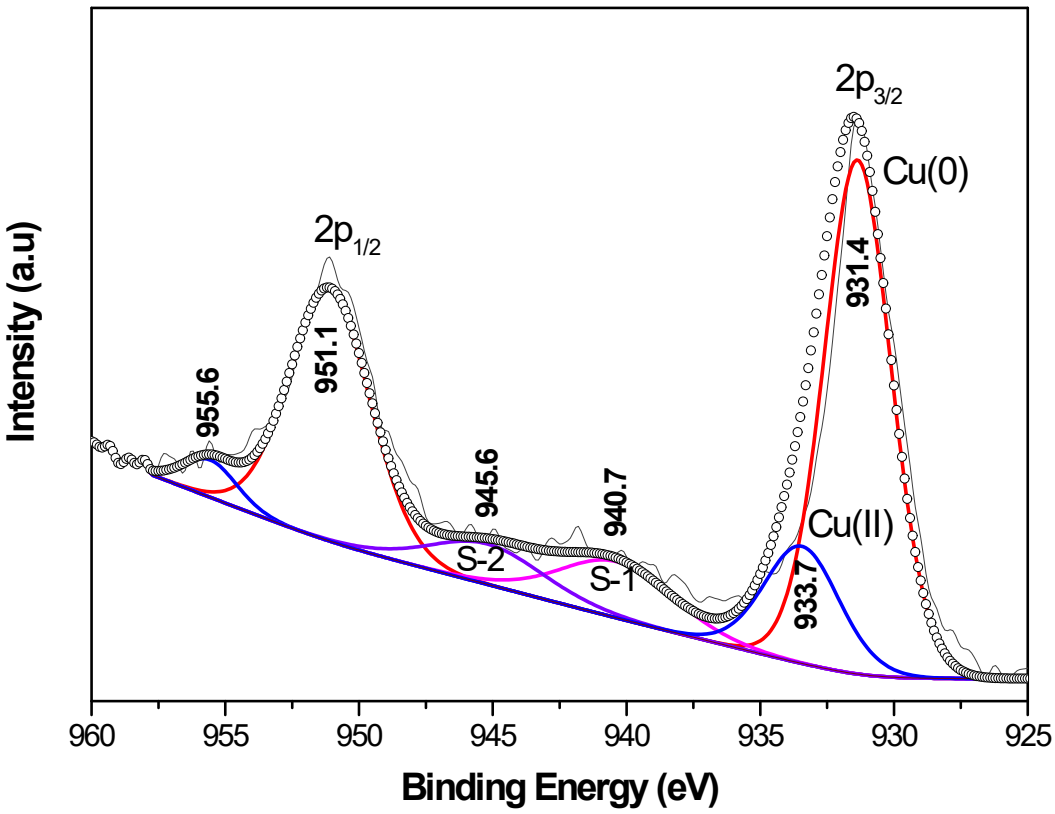

Fig. S33 XPS spectrum of the black residue obtained after catalysis experiment of **4** displaying only the Cu 2p doublet.

4-(phenylethynyl)acetophenone: ^{1}H NMR (300 MHz, $CDCl_3$) δ ppm: 2.62 (s, 3H, $COCH_3$), 7.38 (br, 3H), 7.56 (br, 2H), 7.61 (d, 7.8 Hz, 2H), 7.94 (d, 7.5 Hz, 2H). ^{13}C{^{1}H} NMR (75 MHz, $CDCl_3$) δ ppm: 26.6(CH_3), 88.6, 92.7, 122.7, 128.2, 128.3, 128.4, 128.8, 131.6, 131.7, 136.2, 197.3(C=O).

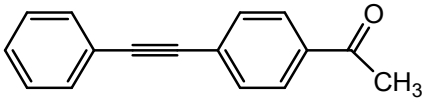

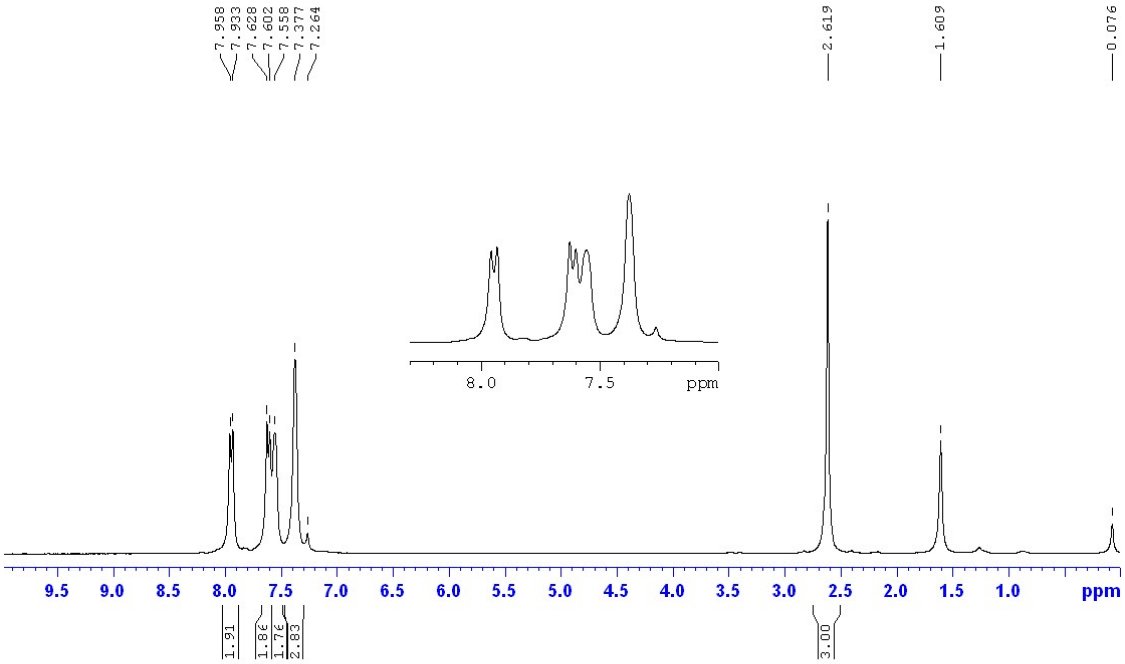

Fig. S34 ^{1}H NMR (300 MHz, $CDCl_3$) of 4-(phenylethynyl)acetophenone.

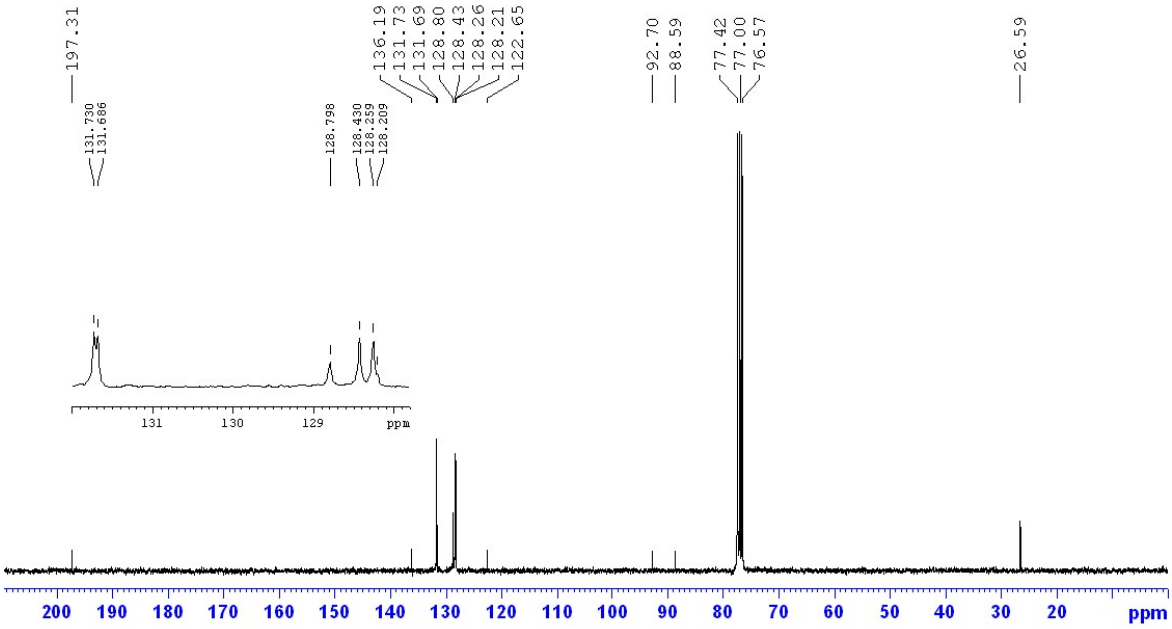

Fig. S35 ^{13}C{^{1}H} NMR (75 MHz, $CDCl_3$) of 4-(phenylethynyl)acetophenone.

4-(phenylethynyl)benzaldehyde: ^{1}H NMR (300 MHz, $CDCl_3$) δ ppm: 7.38-7.39 (m. 3H), 7.56-7.57 (m, 2H), 7.67 (d, 7.8 Hz, 2H), 7.87 (d, 8.1 Hz, 2H), 10.02 (s, 1H, CHO). ^{13}C{^{1}H} NMR (75 MHz, $CDCl_3$) δ ppm: 88.5, 93.4, 122.5, 128.5, 128.9, 129.6, 131.8, 132.1, 135.4, 191.4(C=O).

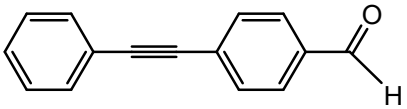

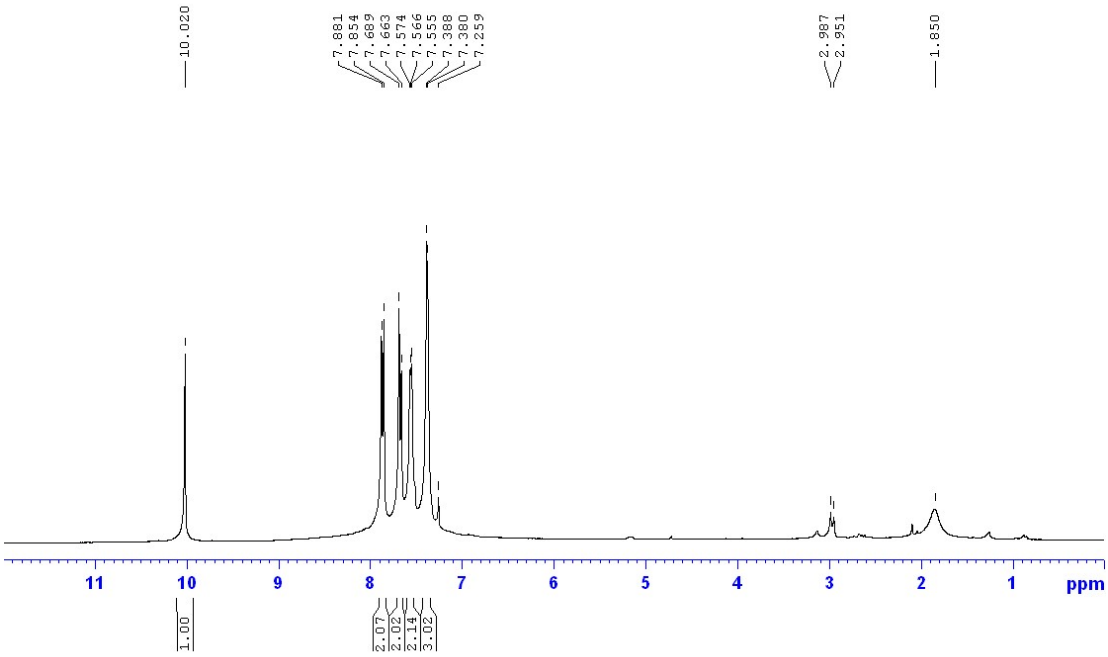

Fig. S36 ^{1}H NMR (300 MHz, $CDCl_3$) of 4-(phenylethynyl)benzaldehyde.

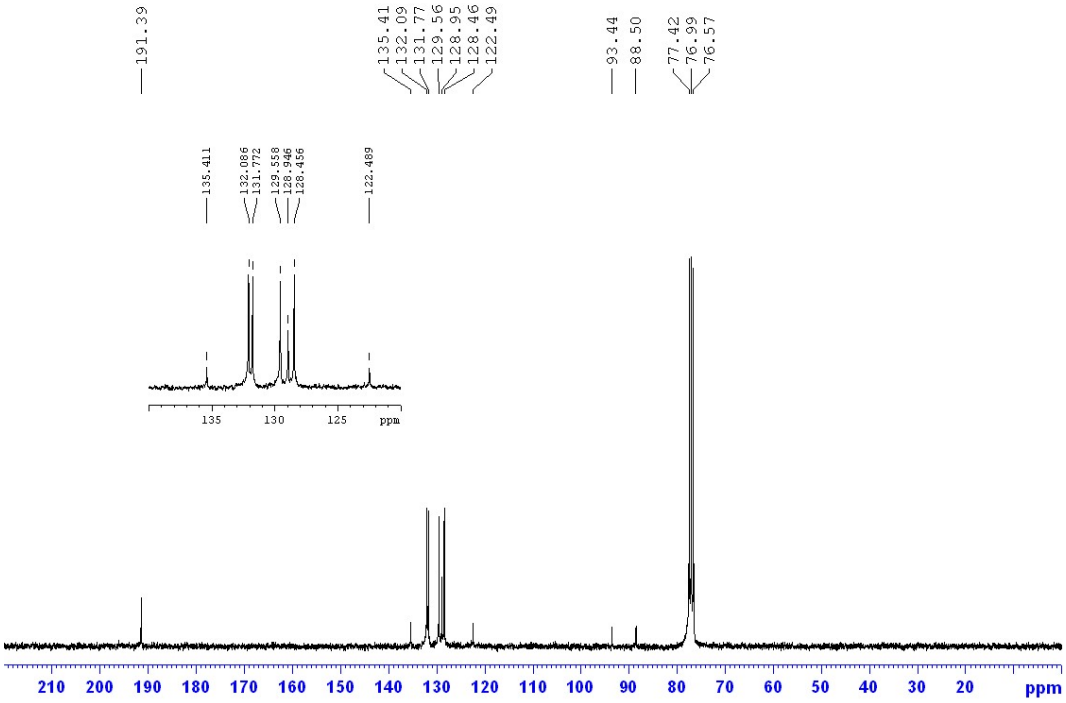

Fig. S37 ^{13}C{^{1}H} NMR (75 MHz, $CDCl_3$) of 4-(phenylethynyl)benzaldehyde.

4-(phenylethynyl)benzoate: ^{1}H NMR (300 MHz, $CDCl_3$) δ ppm: 3.91 (s, 3H, OCH_3), 7.34 (br, 3H), 7.53 (br d, 2H), 7.58 (d, 8.4 Hz, 2H), 7.90 (d, 8.1 Hz, 2H).

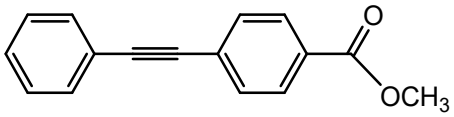

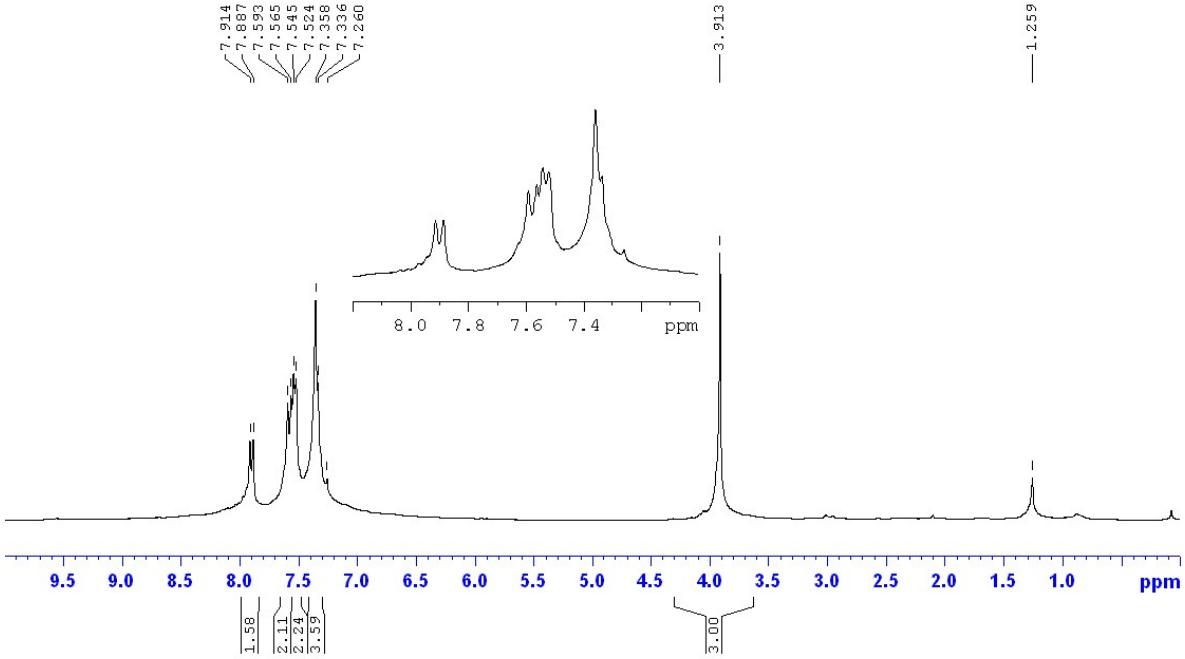

Fig. S38 ^{1}H NMR (300 MHz, $CDCl_3$) of Methyl 4-(phenylethynyl)benzoate.

4-(phenylethynyl)anisole: ^{1}H NMR (300 MHz, $CDCl_3$) δ ppm: 3.78 (s, 3H, OCH_3), 6.78 (d, 9.0 Hz, 2H), 7.34-7.40 (m, 5H), 7.54 (d, 7.5 Hz, 2H).

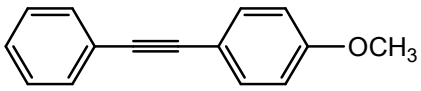

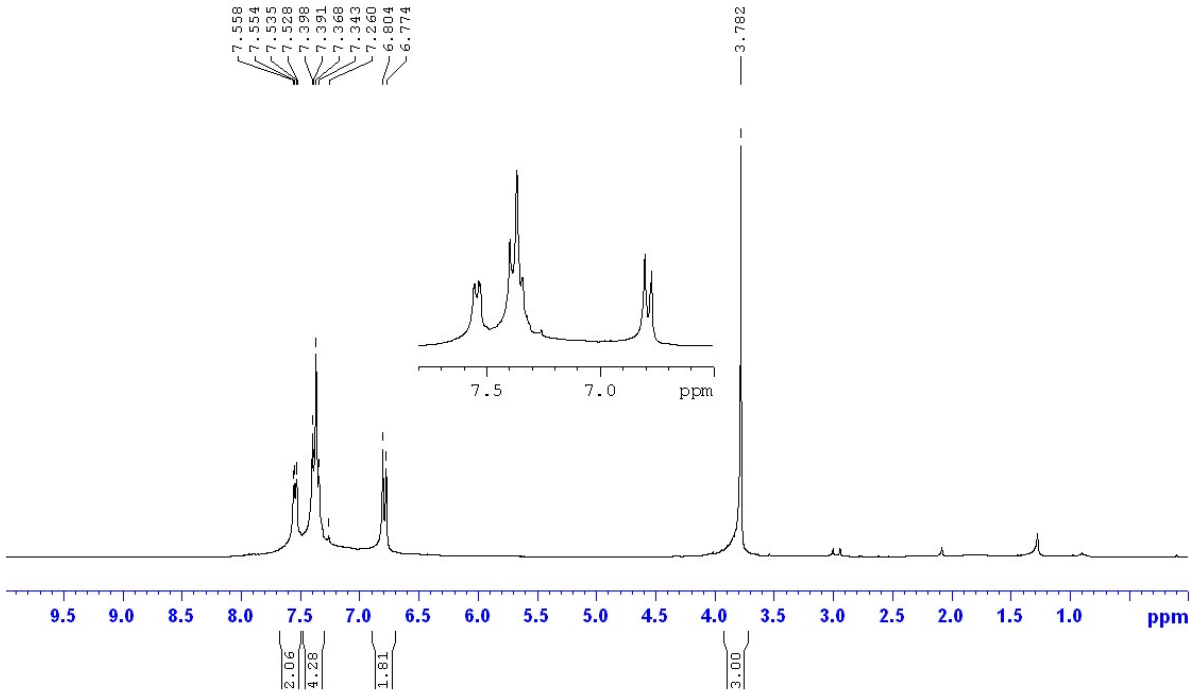

Fig. S39 ^{1}H NMR (300 MHz, $CDCl_3$) of 4-(phenylethynyl)anisole.

1-(phenylethynyl)-4-nitrobenzene: ^{1}H NMR (300 MHz, $CDCl_3$) δ ppm: 7.41 (br, 3H), 7.56-7.57 (br m, 2H), 7.67 (d, 8.7 Hz, 2H), 7.22 (d, 8.4 Hz, 2H). ^{13}C{^{1}H} NMR (75 MHz, $CDCl_3$) δ ppm: 87.5, 94.7, 122.1, 123.6, 125.0, 128.5, 129.3 130.3, 131.8, 132.2, 147.0.

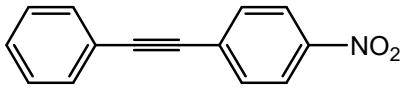

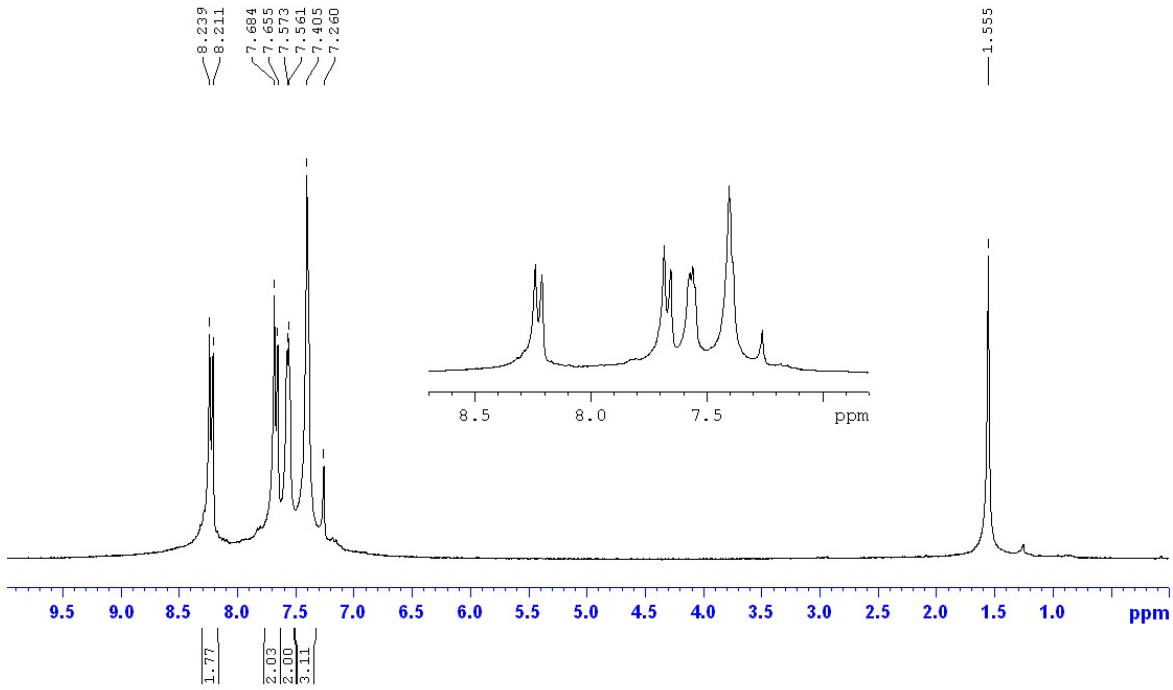

Fig. S40 ^{1}H NMR (300 MHz, $CDCl_3$) of 1-(phenylethynyl)-4-nitrobenzene.

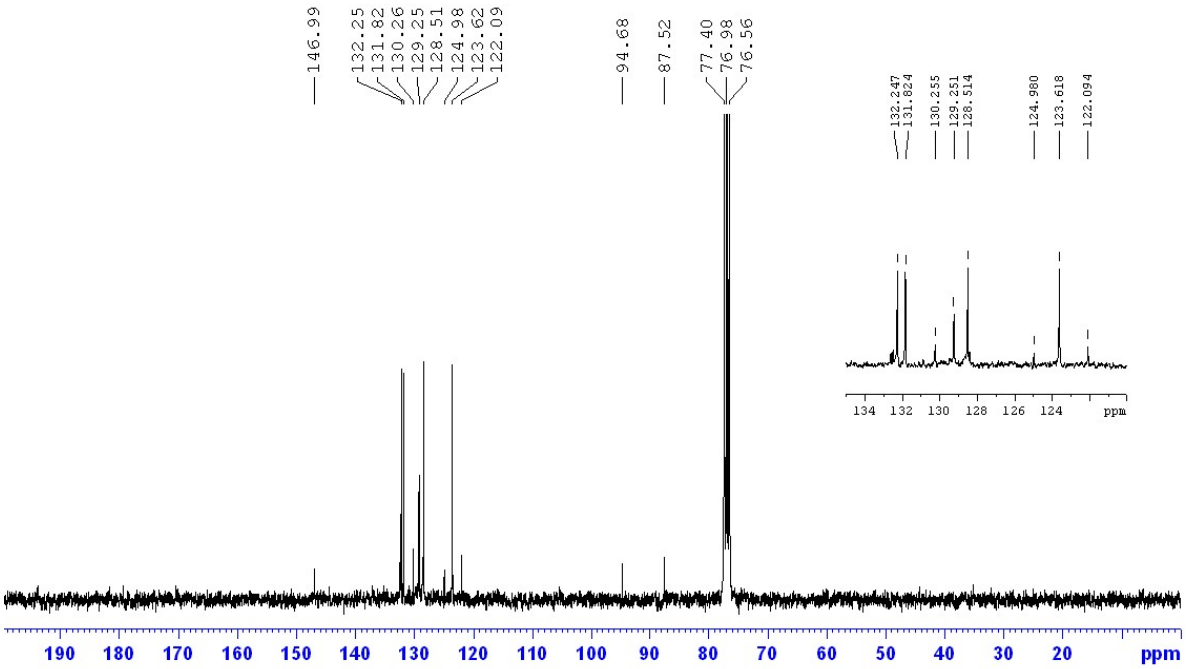

Fig. S41 ^{13}C{^{1}H} NMR (75 MHz, $CDCl_3$) of 1-(phenylethynyl)-4-nitrobenzene.

2-(2-phenylethynyl)pyridine: ^{1}H NMR (300 MHz, $CDCl_3$) δ ppm: 7.22-7.61 (m, 1H), 7.36-7.38 (m, 3H), 7.53 (d, 7.8 Hz, 1H), 7.59-7.62 (m, 2H), 7.65-7.70 (m, 1H), 8.62 (d, 3.3 Hz, 1H). ^{13}C{^{1}H} NMR (75 MHz, $CDCl_3$) δ ppm: 88.6, 89.2. 122.3, 122.7, 127.1, 128.4, 128.9, 129.2, 132.0, 132.5, 136.1, 143.5, 150.0

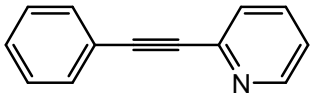

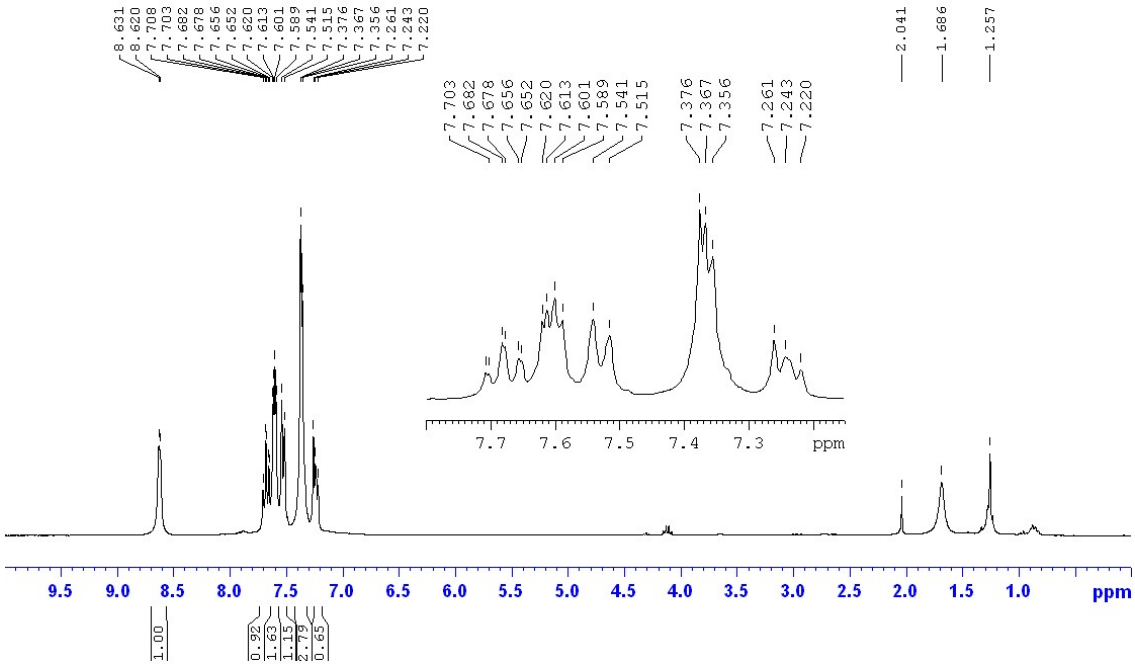

Fig. S42 ^{1}H NMR (300 MHz, $CDCl_3$) of 2-(2-phenylethynyl)pyridine.

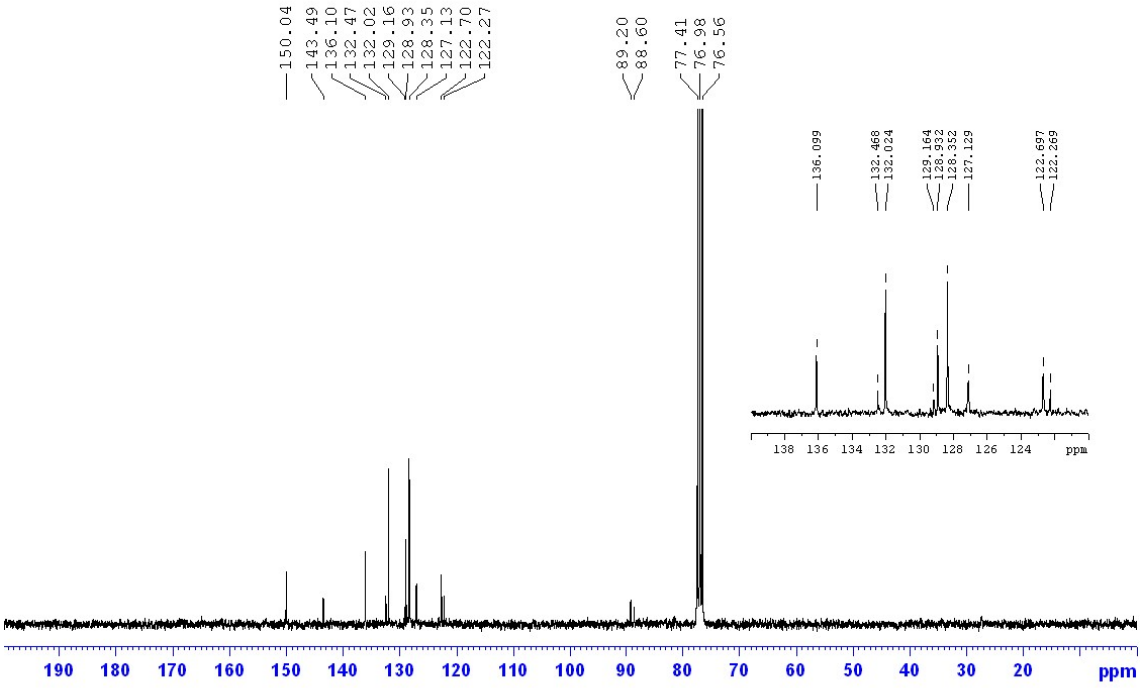

Fig. S43 ^{13}C{^{1}H} NMR (75 MHz, $CDCl_3$) of 2-(2-phenylethynyl)pyridine.

2-(phenylethynyl)thiophene: ^{1}H NMR (300 MHz, $CDCl_3$) δ ppm: 7.01-7.04 (m, 1H), 7.29 (d, 4.5 Hz, 2H), 7.35- 7.36 (br m, 3H), 7.52-7.54 (m, 2H). ^{13}C{^{1}H} NMR (75 MHz, $CDCl_3$) δ ppm: 82.6, 93.0. 123.0, 123.4, 127.1, 127.2, 128.3, 128.4, 129.2, 131.4, 131.9, 132.5

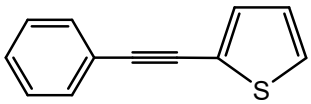

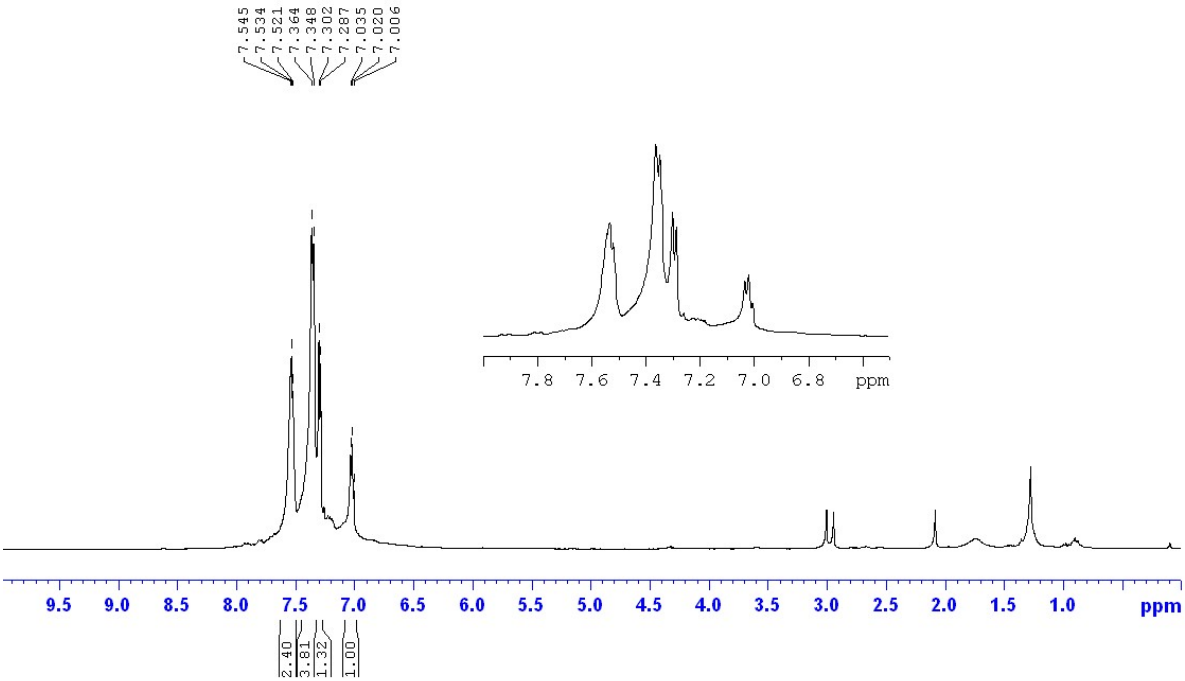

Fig. S44 ^{1}H NMR (300 MHz, $CDCl_3$) of 2-(phenylethynyl)thiophene.

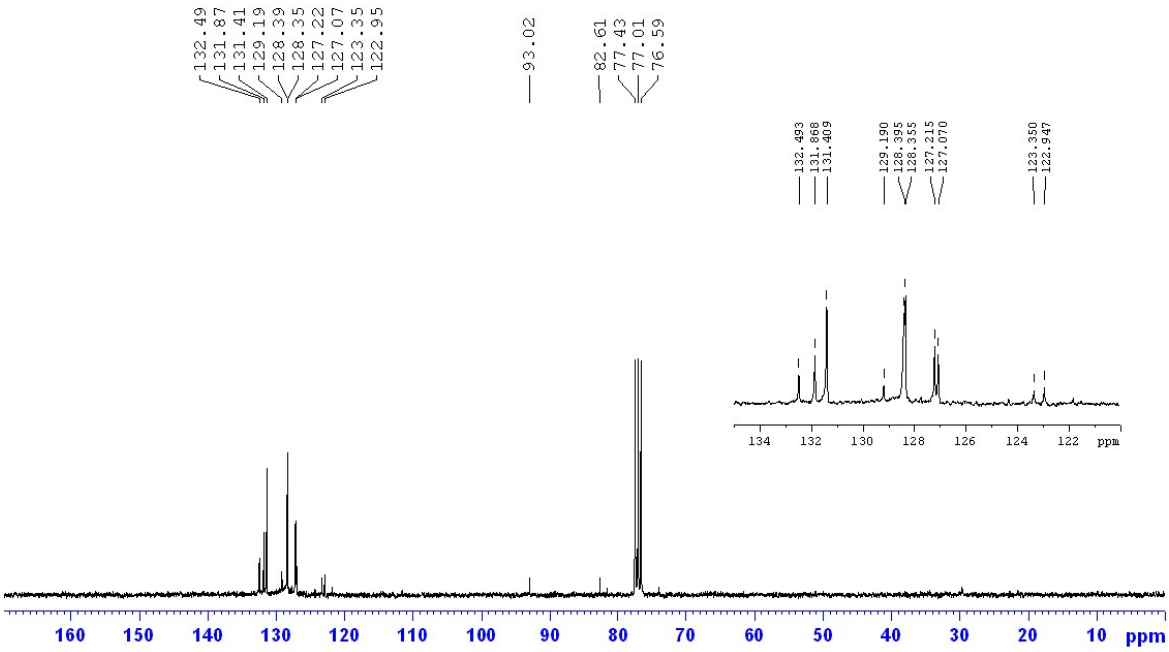

Fig. S45 ^{13}C{^{1}H} NMR (75 MHz, $CDCl_3$) of 2-(phenylethynyl)thiophene.

4-(phenylethynyl)benzonitrile: ^{1}H NMR (300 MHz, $CDCl_3$) δ ppm: 7.38-7.39 (br m. 3H), 7.54-7.56 (m, 2H), 7.62-7.65 (m, 4H). ^{13}C{^{1}H} NMR (75 MHz, $CDCl_3$) δ ppm: 87.7, 93.8, 111.5, 118.5, 122.2, 128.2, 128.5, 129.1, 131.8, 132.1.

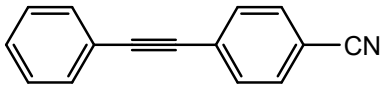

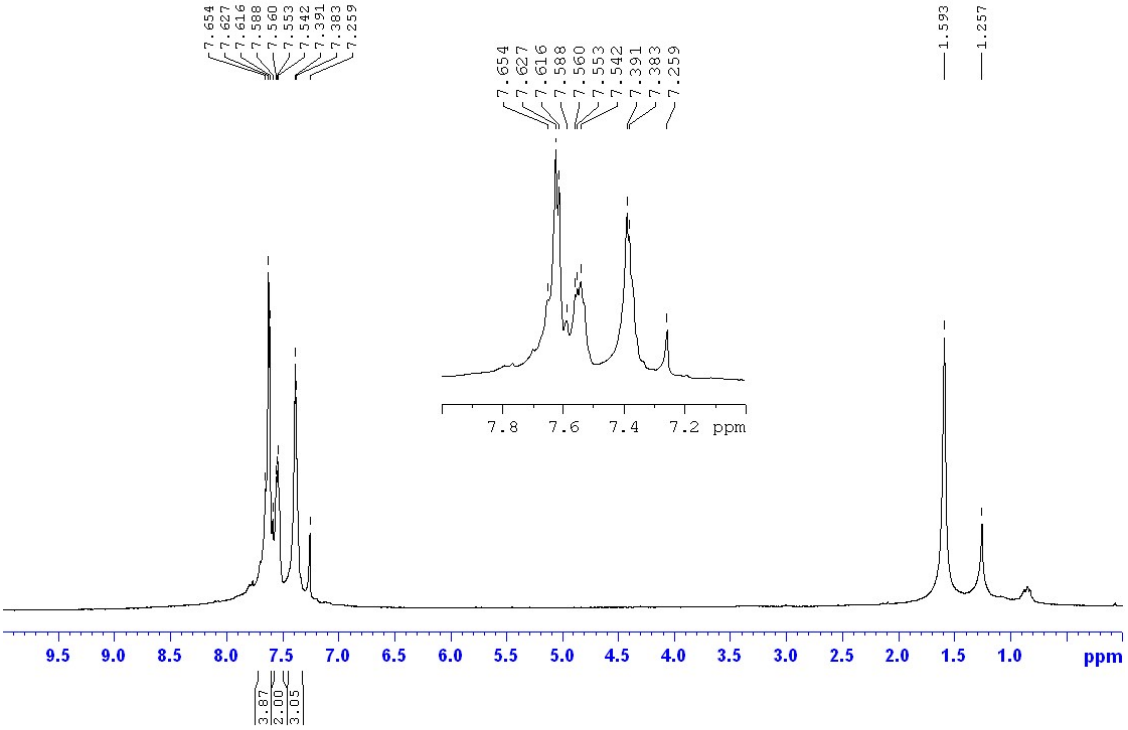

Fig. S46 ^{1}H NMR (300 MHz, $CDCl_3$) of 4-(phenylethynyl)benzonitrile.

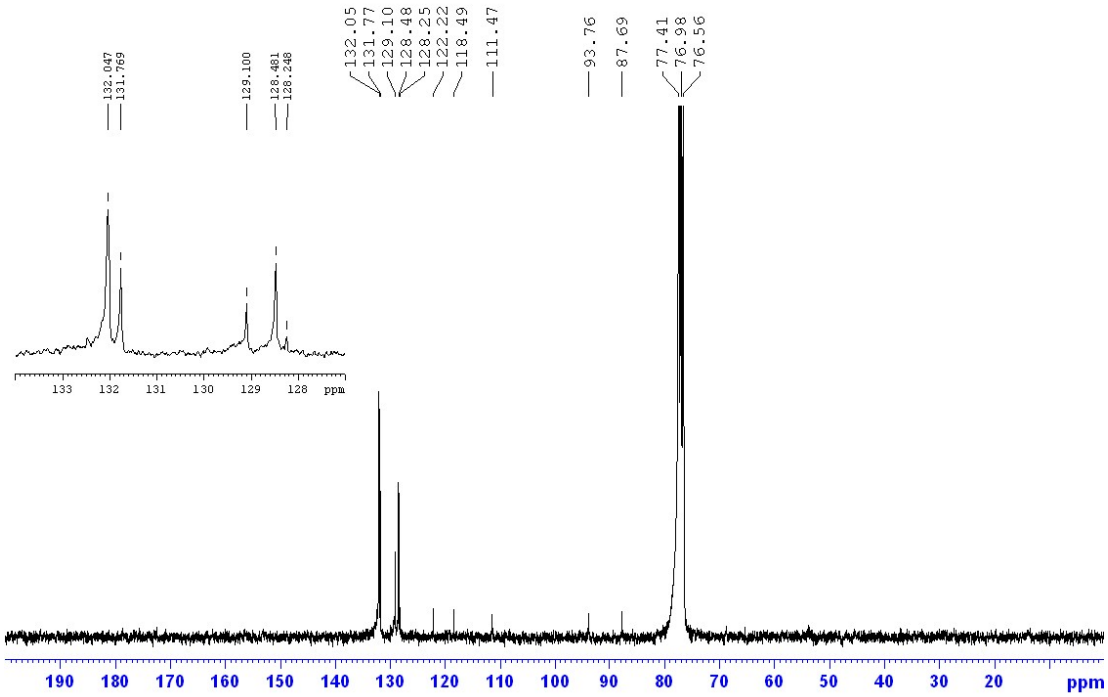

Fig. S47 ^{13}C{^{1}H} NMR (75 MHz, $CDCl_3$) of 4-(phenylethynyl)benzonitrile.